Can assimilation of crowdsourced data in hydrological modelling improve flood prediction?

M. Mazzoleni[1], M. Verlaan[2], L. Alfonso[1], M. Monego[3], D. Norbiato[3], M. Ferri[3] and D.P. Solomatine[1,4]

[1]{UNESCO-IHE Institute for Water Education, Delft, The Netherlands}

[2]{Deltares, Delft, The Netherlands}

[3]{Alto Adriatico Water Authority, Venice, Italy}

[4]{Delft University of Technology, Water Resources Section, Delft, The Netherlands}

Correspondence to: M. Mazzoleni (m.mazzoleni@unesco-ihe.org)

Abstract

Monitoring stations have been used for decades to properly measure hydrological variables and better predict floods. To this end, methods to incorporate these observations into mathematical water models have also being developed. Besides, in recent years the continued technological advances, in combination with the need of involving citizens in participatory processes related to water resources management, have encouraged the increase of citizen science projects around the globe. In turn, this has stimulated the spread of low-cost sensors to allow citizens participating in the collection of hydrological data in a more distributed way than the classic static physical sensors do. However, two main disadvantages of such crowdsourced data are the irregular availability and variable accuracy from sensor to sensor, which makes them, if not discouraging, challenging to use in hydrological modelling. This study aims to demonstrate that streamflow data, derived from crowdsourced water level observations with the characteristics described above, can improve flood prediction if integrated in hydrological models. Two different types of hydrological models, applied to four case studies, are considered. Realistic (albeit synthetic) time series are used to represent crowdsourced data in all case studies. In this study it is found that the data accuracy has much more influence on the model results than the irregular frequency of data availability at which the streamflow data is assimilated. This study demonstrates that data collected by citizens, characterised by being asynchronous and

inaccurate, can still complement traditional networks formed by few accurate, static sensors and improve the accuracy of flood forecasts.

1 Introduction

Observations of hydrological variables measured by physical sensors have been increasingly integrated into mathematical models by means of model updating methods. The use of these techniques allows for the reduction of intrinsic model uncertainty and improves the flood forecasting accuracy (Todini et al., 2005). The main idea behind model updating techniques is to either update model input, states, parameters or outputs as new observations become available (Refsgaard, 1997; WMO, 1992). Input update is the classical method used in operational forecasting as uncertainties of the input data can be considered as the main source of uncertainty (Bergström, 1991; Canizares et al., 1998; Todini et al., 2005). Regarding the state updating, Kalman filtering approaches such as Kalman filter (Kalman, 1960), extended Kalman filter (Aubert et al., 2003; Kalman, 1960; Madsen and Cañizares, 1999; Verlaan, 1998) or Ensemble Kalman filter (EnKF, Evensen, 2006) are ones of the most used when new observations are available.

Due to the complex nature of the hydrological processes, spatially and temporally distributed measurements are needed in the model updating procedures to ensure a proper flood prediction (Clark et al., 2008; Mazzoleni et al., 2015; Rakovec et al., 2012). However, traditional physical sensors require proper maintenance and personnel which can be very expensive for a vast network. For this reason, the technological improvement led to the spread of low-cost sensors used to measure hydrological variables, such as water level or precipitation, in a more distributed way. The main advance of using these type of sensors, defined in the following as "social sensor", is that they can be used not only by technicians but also by regular citizens, and that due to their reduced cost a more spatially distributed coverage can be achieved. The idea of designing these alternative networks of low-cost social sensors and using the obtained crowdsourced observations is the base of the EU-FP7 WeSenseIt project (2012-2016), which also sponsors this research. Various other projects have also been initiated in order to assess the usefulness of crowdsourced observations inferred by low-cost sensors owned by citizens. For instance, in the project CrowdHydrology (Lowry and Fienen, 2013), a method to monitor stream stage at designated gauging staffs using crowdsource-based text messages of water levels is developed using untrained observers. Cifelli et al. (2005) described a community-based

network of volunteers (CoCoRaHS), engaged in collecting precipitation measurements of rain, hail and snow. An example of hydrological monitoring, established in 2009, of rainfall and streamflow values within the Andean ecosystems of Piura, Peru, based on citizen observations is reported in Célleri et al. (2009). Degrossi et al. (2013) used a network of wireless sensors in order to map the water level in two rivers passing by Sao Carlos, Brazil. Recently, the iSPUW Project was initiated to integrate data from advanced weather radar systems, innovative wireless sensors and crowdsourcing of data via mobile applications, in order to better predict flood events the Dallas-Fort Worth Metroplex urban water systems (ISPUW, 2015; Seo et al., 2014). Other examples of crowdsourced water-related information include the so-called Crowdmap platform for collecting and communicating the information about the floods in Australia in 2011 (ABC, 2011), and informing citizens about the proper time for water supply in an intermittent water system (Alfonso, 2006; Au et al., 2000; Roy et al., 2012). Wehn et al. (2015) stressed the importance and need of public participation in water resources management to ensure citizens' involvement in the flood management cycle. A detailed and interesting review of the examples of citizen science applications in hydrology and water resources science is provided by Buytaert et al. (2014). In this review paper, the potential of citizen science, based on robust, cheap, and low-maintenance sensing equipment, to complement more traditional ways of scientific data collection for hydrological sciences and water resources management is explored. In order to study the challenges and opportunities in the integration of hydrologically-oriented citizen science in water resources management, four case studies are considered.

The traditional hydrological observations from physical sensors have a well-defined structure in terms of frequency and accuracy. On the other hand, crowdsourced observations are provided by citizens with varying experience of measuring environmental data and little connections between each other, and the consequence is that the low correlation between the measurements might be observed. So far, in operational hydrology practice, the added value of crowdsourced data it is not integrated into the forecasting models but just used to compare the model results with the observations in a post-event analysis. This can be related to the intrinsic variable accuracy, due to the lack of confidence in the data quality from these heterogeneous sensors, and the variable life-span of the crowdsourced observations.

Regarding data quality, Bordogna et al. (2014) and Tulloch and Szabo (2012) stated that quality control mechanisms should consider contextual conditions to deduce indicators about reliability (expertise level), credibility (volunteer group) and performance of volunteers such as accuracy,

completeness and precision level. Bird et al. (2014) addressed the issue of data quality in conservation ecology by means of new statistical tools to assess random error and bias. Cortes et al. (2014) evaluated data quality by distinguishing the in-situ data collected between volunteers and technicians and comparing the most frequent value reported at a given location. With in-situ exercises, it might be possible to have an indication of the reliability of data collected. However, this approach is not enough at operational level to define accuracy in data quality. For this reason, to estimate observation accuracy in real-time one possible approach could be to filter out the measurements following a geographic approach which defines semantic rules governing what can occur at a given location (e.g. Vandecasteele and Devillers, 2013). Another approach could be to compare measurements collected within a predefined time-window in order to calculate the most frequent value, the mean and the standard deviation.

Regarding the variable life-span, crowdsourced observations can be defined as *asynchronous* because they do not have predefined rules about the arrival frequency (the observation might be sent just once, occasionally or at irregular time steps which can be smaller than the model time step) and accuracy. In a recent paper, Mazzoleni et al. (2015) presented results of the study of the effects of distributed synthetic streamflow observations having synchronous intermittent temporal behaviour and variable accuracy in a semi-distributed hydrological model. It has been shown that the integration of distributed uncertain intermittent observations with single measurements coming from physical sensors would allow for the further improvements in model accuracy. However, we have not considered the possibility that the asynchronous observations might be coming at the moments not coordinated with the model time steps. A possible solution to handle asynchronous observations in time with EnKF is to assimilate them at the moments coinciding with the model time steps (Sakov et al., 2010). However, as these authors mention, this approach requires the disruption of the ensemble integration, the ensemble update and a restart, which may not feasible for large-scale forecasting applications. Continuous approaches, such as 3D-Var or 4D-Var methods, are usually implemented in oceanographic modelling in order to integrate asynchronous observations at their corresponding arrival moments (Derber and Rosati, 1989; Huang et al., 2002; Macpherson, 1991; Ragnoli et al., 2012). In fact, oceanographic observations are commonly collected at not pre-determined, or asynchronous, times. For this reason, in variational data assimilation, the past asynchronous observations are simultaneously used to minimize the cost function that measures the weighted difference between background states and observations over the time interval, and identify the best estimate of the initial state condition (Drecourt, 2004; Ide et al., 1997; Li and Navon, 2001). In

addition to the 3D-Var and 4D-Var methods, Hunt et al. (2004) proposed a Four Dimensional Ensemble Kalman Filter (4DEnKF) which adapts EnKF to handle observations that have occurred at non-assimilation times. In this method the linear combinations of the ensemble trajectories are used to quantify how well a model state at the assimilation time fits the observations at the appropriate time. Furthermore, for linear dynamics 4DEnKF is equivalent to instantaneous assimilation of the measured data (Hunt et al., 2004). Similarly to 4DEnKF, Sakov et al. (2010) proposed a modification of the EnKF, the Asynchronous Ensemble Kalman Filter (AEnKF), to assimilate asynchronous observations (Rakovec et al., 2015). Contrary to the EnKF, in the AEnKF current and past observations are simultaneously assimilated at a single analysis step without the use of an adjoin model. Yet another approach to assimilate asynchronous observations in models is the so-called First-Guess at the Appropriate Time (FGAT) method. Like in 4D-Var, the FGAT compares the observations with the model at the observation time. However, in FGAT the innovations are assumed constant in time and remain the same within the assimilation window (Massart et al., 2010). Having reviewed all the described approaches, in this study we have decided to use a straightforward and pragmatic method, due to the linearity of the hydrological models implemented in this study, to assimilate the asynchronous crowdsourced observations.

The main objective of this novel study is to assess the potential use of crowdsourced data within hydrological modelling. In particular, the specific objectives of this study are to a) assess the influence of different arrival frequency of the crowdsourced data and their related accuracy on the assimilation performances for a single social sensor; b) to integrate the distributed low-cost social sensors with a single physical sensor to assess the improvement in the streamflow prediction performances in an early warning system. The methodology is applied in the Brue (UK), Sieve (Italy), Alzette (Luxemburg) and Bacchiglione (Italy) catchments, considering lumped and semi-distributed hydrological models respectively. Due to the fact that data derived from social sensors observations of water level are not available in the Brue, Sieve and Alzette catchments while in the Bacchiglione catchment the sensors are being recently installed, the synthetic time series, asynchronous in time and with random accuracy, that imitate the crowdsourced data, are generated and used.

The study is organized as follows. Firstly, the case studies, the crowdsourced data and the datasets used are presented. Secondly, the hydrological models, the procedure used to integrate

the crowdsourced data and the set of experiments are reported. Finally, the results, discussion, and conclusions are presented.

2 Sites locations and data

2.1 Case studies

Four different case studies are chosen to validate the obtained results for areas having diverse topographical and hydrometeorological features and represented by two different hydrological models. The Brue, Sieve and Alzette catchments are considered because of the availability of precipitation and streamflow data, while the Bacchiglione catchment is one of the official case studies of the WeSenseIt Project (Huwald et al., 2013), which is funding this research.

2.1.1 Brue catchment

The first case study is located in the Brue catchment (Figure 1), in Somerset, with a drainage area of about 135 km^2 at the catchment outlet in Lovington. Using the SRTM DEM with the 90m resolution it is possible to derive the topographical characteristics, streamflow network and the consequent time of concentration, by means of the Giandotti equations (Giandotti, 1933), which is about 10 hours. The hourly precipitation (49 rainfall stations) and streamflow data used in this study are supplied by the British Atmospheric Data Centre from the HYREX (Hydrological Radar Experiment) project (Moore et al., 2000; Wood et al., 2000). The average precipitation value in the catchment is estimated using the Ordinary Kriging (Matheron, 1963).

2.1.2 Sieve catchment

The second case study is the Sieve catchment (Figure 1), a tributary of the Arno River, is located in the Central Italian Apennines, Italy. The catchment has a drainage area of about 822km^2 with the length of 56 km and it covers mostly hills and mountainous areas with an average elevation of 470 m above sea level. The time of concentration of the Sieve catchment is about 12 hours. Hourly streamflow data are provided by the Centro Funzionale di Monitoraggio Meteo Idrologico-Idralico of the Tuscany Region at the outlet section of the catchment at Fornacina. The mean areal precipitation is calculated by Thiessen polygon method using 11 rainfall stations (Solomatine and Dulal, 2003).

2.1.3 Alzette catchment

The Alzette catchment is located in the large part of the Grand-Duchy in Luxembourg. The drainage area of the catchment is about 288km^2 and the river has a length of 73 km along France and Luxembourg. The catchment covers cultivated land, grassland, forestland and urbanized land (Fenicia et al., 2007). Thiessen polygon method is used for averaging the series at the individual stations and calculate hourly rainfall series (Fenicia et al., 2007), while streamflows data are available measured at the Hesperange gauging station.

2.1.4 Bacchiglione catchment

The last case study is the upstream part of the Bacchiglione River basin, located in the North-East of Italy, and tributary of the River Brenta which flows into the Adriatic Sea at the South of the Venetian Lagoon and at the North of the River Po delta. The study area has an overall extent and river length of about 400 km2 and 50 km (Ferri et al., 2012). The main urban area located in the downstream part of the study area is Vicenza. The analysed part of the Bacchiglione River has four main tributaries. On the Western side, the confluences with the Bacchiglione are the Leogra, the Orolo and the Retrone River, whose junction is located in the urban area itself. In Figure 2 the Retrone River it is not shown since it does not influence the water level measured at the gauged station of Vicenza (Ponte degli Angeli in Figure 2). On the Eastern side there is the Timonchio River (see Figure 2). The Alto Adriatico Water Authority (AAWA) has implemented an Early Warning System to properly forecast the possible future flood events.

2.2 Crowdsourced data

Social sensors can be used by citizens to provide crowdsourced distributed hydrological observations such as precipitation and water level. An example of these sensors can be a staff gauge, connected to a QR code, on which citizens can read water level indication and send observations via a mobile phone application. Another example is the collection of rainfall data via lab-generated videos (Alfonso et al., 2015). Recently, within the activities of the WeSenseIt Project (Huwald et al., 2013), one physical sensor and three staff gauges complemented by a QR code were installed in the Bacchiglione River to measure the water level. In particular, the physical sensor is located at the outlet of the Leogra catchment while the three social sensors are located at the Timonchio, Leogra and Orolo catchments outlet respectively (see Figure 2).

It is worth noting that, in most of the cases, it is difficult to directly assimilate water level observations within hydrological models. However, it is highly unrealistic to assume that citizens might observe streamflow directly. For this reason, crowdsourced *observations* of water level are used to calculate crowdsourced *data* (CSD) of streamflow, by means of rating curves assessed for the specific river location, which can be easily assimilated in hydrological models. It is because of both the uncertainty in rating curve estimation at the social sensor location and the error in the water level measurements that CSD has such low and variable accuracy when compared to streamflow data estimated from classic physical sensors. The CSD is then assimilated within mathematical models as described in Figure 3 ("Overall information flow").

In most hydrological applications, streamflow data from physical sensors are derived (and integrated into hydrological models) at a regular, synchronous, time steps. However, due to the fact that crowdsourced water level observations are obtained by diverse type of citizens at different random moments, from the modelling viewpoint CSD have three main characteristics: a) irregular arrival frequency (asynchronicity); b) random accuracy; c) random number of CSD received within two model time steps. Due to the fact that streamflow CSDs are not available in case studies at the moment of this study, realistic synthetic CSD with these characteristics are generated ("Considered information flow" in Figure 3).

For the Brue, Sieve and Alzette catchments observed hourly streamflow data at the catchments outlet are interpolated to represent CSD coming at arrival frequency higher than hourly. For the Bacchiglione catchment, synthetic hourly CSDs of streamflow are calculated using measured precipitation recorded during the considered flood events (post-event simulation) as input in the hydrological model of the Bacchiglione catchment. A similar approach, termed "observing system simulation experiment" (OSSE), is commonly used in meteorology to estimate synthetic "true" states and measurements by introducing random errors in the state and measurement equations (Arnold and Dey, 1986; Errico et al., 2013; Errico and Privé, 2014). OSSEs have the advantage of making it possible to directly compare estimates to "true" states and they are often used for validating DA algorithms.

Further details and assumptions regarding the characteristics of CSD and related uncertainty are provided in the next sections.

2.3 Datasets

Three flood events for each one of the four described catchments are considered to assess the assimilation of CSD in hydrological modelling.

For the Brue catchment, a 2 years' time series (June 1994 to May 1996) of observed streamflow and precipitation data are available for model calibration and validation. On the other hand, for the Sieve catchment only 3 months of hourly runoff, streamflow and precipitation data (December 1959 to February 1960) are available (Solomatine and Shrestha, 2003). For the Alzette catchment, two-year hourly data (July 2000 to June 2002) are used for the model calibration and validation (Fenicia et al., 2007). For these catchments, the observed precipitation values are treated as the "perfect forecasts" and are fed into the hydrological model.

For the Bacchiglione catchment, three flood events occurred in 2013, 2014 and 2016 are considered. In particular, the one of 2013 had high intensity and resulted in several traffic disruptions at various locations upstream Vicenza. For flood forecasting, AAWA uses the 3-day weather forecast as the input to the hydrological model. In all the case studies, the observed values of streamflow at the catchment outlet (Ponte degli Angeli for the Bacchiglione) are used to assess the performance of the hydrological model.

3 Methodology

3.1 Hydrological modelling

3.1.1 Lumped model

A lumped conceptual hydrological model is implemented to estimate the streamflow hydrograph at the outlet section of the Brue, Sieve and Alzette catchments. The choice of the model is based on previous studies performed on the Brue catchment (Mazzoleni et al., 2015). Direct runoff is used as input in the conceptual model and assessed by means of the Soil Conservation Service Curve Number (SCS-CN) method (Mazzoleni et al., 2015). The average value of CN within the catchment is calibrated by minimizing the difference between the simulated volume and observed quickflow, using the method proposed by Eckhardt (2005), at the outlet section.

The main module of the hydrological model is based on the Kalinin-Milyukov-Nash (KMN), Szilagyi and Szollosi-Nagy (2010), equation:

$$Q_t = \frac{1}{k} \cdot \frac{1}{(n-1)!} \int_{t_0}^{t} \left(\frac{\tau}{k} \right)^{n-1} \cdot e^{-\tau/k} \cdot I(t-\tau) \cdot d\tau \qquad (1)$$

where I is the model forcing (in this case direct runoff), n (number of storage elements) and k (storage capacity expressed in hours) are the two model parameters and Q is the model output (streamflow). In this study, the parameter k is assumed as a linear function between the time of concentration, assessed using the Giandotti equation (Giandotti, 1933) and a coefficient c_k. The discrete state-space system of Eq. (1) derived by Szilagyi and Szollosi-Nagy (2010) is used in this study to apply the data assimilation (DA) approach (Mazzoleni et al., 2015, 2016).

The model calibration is performed maximizing the NSE and correlation between the simulated and observed value of streamflow, at the outlet point of the Brue, Sieve and Alzette catchments, using historical time series. The results of the calibration provided a value of the parameters n and c_k equal to 4 and 0.026, 1 and 0.0055, and 1 and 0.00064 for the Brue, Sieve and Alzette catchments respectively.

3.1.2 Semi-distributed model

The hydrological and routing models used in this study are based on the early warning system implemented by the AAWA and described in Ferri et al. (2012). One of the goals of this study, in the framework of the WeSenseIt Project, is to test our methodology using synthetic CSD in the existing early warning system implemented by AAWA on the Bacchiglione catchment.

In the schematization of the Bacchiglione catchment, the location of physical and social sensors corresponds to the outlet section of three main sub- catchments, Timonchio, Leogra and Orolo, while the remaining sub-catchments are considered as inter-catchment. For both sub-catchments and inter-catchments, a conceptual hydrological model, described below, is used to estimate the outflow hydrograph. The outflow hydrograph of the three main sub-catchments is considered as upstream boundary conditions of a routing model used to propagate the flow up to the catchment outlet (see Figure 2), while the outflow from the inter-catchment is considered as internal boundary condition to account for their corresponding drained area. In the following, a brief description of the main components of the hydrological and routing models is provided.

The input for the hydrological model consists of precipitation only. The hydrological response of the catchment is estimated using a hydrological model that considers the routines for runoff generation and a simple routing procedure. The processes related to runoff generation (surface, sub-surface and deep flow) are modelled mathematically by applying the water balance to a control volume representative of the active soil at the sub-catchment scale. The water content S_w in the soil is updated at each calculation step dt using the following balance equation:

$$S_{w,t+dt} = S_{w,t} + P_t - R_{sur,_t} - R_{sub,_t} - L_t - E_{\mathrm{T},t} \tag{2}$$

where P and E_T are the components of precipitation and evapotranspiration, while R_{sur}, R_{sub} and L are the surface runoff, sub-surface runoff and deep percolation model states respectively (see Figure 2). The surface runoff is expressed by the equation based on specifying the critical threshold beyond which the mechanism of dunnian flow (saturation excess mechanism) prevails:

$$R_{sur,_t} = \begin{cases} C \cdot \left(\dfrac{S_{w,t}}{S_{w,\max}} \right) \cdot P_t \Rightarrow P_t \le f = \dfrac{S_{w,\max} \cdot \left(S_{w,\max} - S_{w,t} \right)}{\left(S_{w,\max} - C \cdot S_{w,t} \right)} \\ P_t - \left(S_{w,\max} - S_{w,t} \right) \Rightarrow P_t > f \end{cases}. \tag{3}$$

where C is a coefficient of soil saturation obtained by calibration, and $S_{w,max}$ is the content of water at saturation point which depends on the nature of the soil and on its use.

The sub-surface flow is considered proportional to the difference between the water content $S_{w,t}$ at time t and that at soil capacity S_c:

$$R_{sub,t} = c \cdot \left(S_{w,t} - S_c \right). \tag{4}$$

while the estimated deep flow is evaluated according to the expression proposed by Laio et al. (2001):

$$L_t = \frac{K_s}{e^{\beta \cdot \left(1 - \frac{S_c}{S_{w,\max}} \right)} - 1} \cdot \left(e^{\beta \cdot \left(\frac{S_{w,t} - S_c}{S_{w,\max}} \right)} - 1 \right). \tag{5}$$

where, K_s is the hydraulic conductivity of the soil in saturation conditions, β is a dimensionless exponent characteristic of the size and distribution of pores in the soil. The evaluation of the real evapotranspiration is performed assuming it as a function of the water content in the soil

and potential evapotranspiration, calculated using the formulation of Hargreaves and Samani (1982).

Knowing the values of R_{sur}, R_{sub} and L, it is possible to model the surface Q_{sur}, sub-surface Q_{sub} and deep flow Q_g routed contributes according to the conceptual framework of the linear reservoir at the closing section of the single sub-catchment. In particular, in case of Q_{sur} the value of the parameter k, which is a function of the residence time in the catchment slopes, is estimated relating the velocity to the average slopes length L. However, one of the challenges is to properly estimate such velocity, which should be calculated for each flood event (Rinaldo and Rodriguez-Iturbe, 1996). According to Rodríguez-Iturbe et al. (1982), this velocity is a function of the effective rainfall intensity and the event duration. In this study, the estimation of the surface velocity is performed using the relation between velocity and intensity of rainfall excess proposed in Kumar et al. (2002), to then estimate the average travel time and the consequent parameter k. However, this formulation is applied in a lumped way for a given sub-catchment. As reported in McDonnell and Beven (2014), more reliable and distributed models should be used to reproduce the spatial variability of the residence times over time within the catchment. That is why, in the advanced version of the model implemented by AAWA, in each sub-catchment the runoff propagation is carried out according to the geomorphological theory of the hydrologic response. The overall catchment travel time distributions is considered as nested convolutions of statistically independent travel time distributions along sequentially connected, and objectively identified, smaller sub-catchments. The correct estimation of the residence time should be derived considering the latest findings reported in McDonnell and Beven (2014). Regarding Q_{sub} and Q_g, the value of k is calibrated comparing the observed and simulated streamflow at Vicenza.

In the early warning system implemented by AAWA in the Bacchiglione catchment, the flood propagation along the main river channel is represented by a one-dimensional hydrodynamic model, MIKE 11 (DHI, 2005). This model solves the Saint Venant Equations for unsteady flow based on an implicit finite difference scheme proposed by Abbott and Ionescu (1967). However, in order to reduce the computational time required by the analysis performed in this study MIKE11 is replaced by a Muskingum-Cunge model (see, e.g. Todini 2007), considering rectangular river cross-sections for the estimation of hydraulic radios, wave celerities and other hydraulic variables.

Calibration of the hydrological and hydrodynamic model parameters is performed by AAWA, and described in Ferri et al. (2012), considering the time series of precipitation from 2000 to 2010 in order to minimize the root mean square error between observed and simulated values of water level at Ponte degli Angeli gauged station. In order to stay as close as possible to the early warning system implemented by AAWA, we used the same calibrated model parameters proposed by Ferri et al. (2012).

3.2 Data assimilation procedure

3.2.1 Kalman Filter

In Data Assimilation (DA) it is typically assumed that the dynamic system can be represented in the state-space as follows:

$$\mathbf{x}_t = M(\mathbf{x}_{t-1}, \vartheta, I_t) + w_t \qquad w_t \sim N(0, \mathbf{S}_t). \tag{6}$$

$$\mathbf{z}_t = H(\mathbf{x}_t, \vartheta) + v_t \qquad v_t \sim N(0, R_t). \tag{7}$$

where, $\mathbf{x}_t$ and $\mathbf{x}_{t-1}$ are state vectors at time t and t-1, M is the model operator that propagates the states $\mathbf{x}$ from its previous condition to the new one as a response to the inputs I_t, while H is the operator which maps the model states into output $\mathbf{z}_t$. The system and measurements errors w_t and v_t are assumed to be normally distributed with zero mean and covariance $\mathbf{S}$ and R. In a hydrological modelling system, these states can represent the water stored in the soil (soil moisture, groundwater) or on the earth surface (snow pack). These states are one of the governing factors that determine the hydrograph response to the inputs into the catchment.

For the linear systems used in this study, the discrete state-space system of Eq. (1) can be represented as follows (Szilagyi and Szollosi-Nagy, 2010):

$$\mathbf{x}_t = \mathbf{\Phi}\mathbf{x}_{t-1} + \mathbf{\Gamma} I_t + w_t . \tag{8}$$

$$Q_t = \mathbf{H}\mathbf{x}_t + v_t . \tag{9}$$

where t is the time step, $\mathbf{x}$ is vector of the model states (stored water volume in m^3), $\mathbf{\Phi}$ is the state-transition matrix (function of the model parameters n and k), $\mathbf{\Gamma}$ is the input-transition matrix, $\mathbf{H}$ is the output matrix, and I and Q are the input (forcing) and model output (streamflow in this case). For example, for n=3 the matrix $\mathbf{H}$ is expressed as $\mathbf{H} = \begin{bmatrix} 0 & 0 & k \end{bmatrix}$. Expressions for matrices $\mathbf{\Phi}$ and $\mathbf{\Gamma}$ can be found in Szilagyi and Szollosi-Nagy (2010).

For the Bacchiglione model, the preliminary sensitivity analysis on the model states (soil content S and the storage water x_{sur}, x_{sub} and x_L related to Q_{sur}, Q_{sub} and Q_g) is performed in order to decide on which of the states to update. The results of this analysis (shown in the next section) pointed out that the stored water volume x_{sur} (estimated using Eq. (8) with n=1, H=k and I_t replaced by R_{sur}) is the most sensitive state and for this reason we decided to update only this state.

The Kalman Filter (KF, Kalman, 1960) is a mathematical tool which allows estimating, in an efficient computational (recursive) way, the state of a process which is governed by a linear stochastic difference equation. KF is optimal under the assumption that the error in the process is Gaussian; in this case KF is derived by minimizing the variance of the system error (error in state) assuming that the model state estimate is unbiased. In an attempt to overcome these limitations, various variants of the Kalman filter, such as the extended Kalman filter (EKF), unscented Kalman filter and ensemble Kalman filter (EnKF) have been proposed.

Kalman filter procedure can be divided in two steps, namely forecast equations, (Eqs. (10) and (11)), and update (or analysis) equations (Eqs. (12), (13) and (14)):

$$\mathbf{x}_t^- = \mathbf{\Phi}\mathbf{x}_{t-1}^+ + \mathbf{\Gamma}\mathbf{I}_t . \tag{10}$$

$$\mathbf{P}_t^- = \mathbf{\Phi}\mathbf{P}_{t-1}^+\mathbf{\Phi}^T + \mathbf{S} . \tag{11}$$

$$\mathbf{K}_t = \mathbf{P}_t^-\mathbf{H}^T\left(\mathbf{H}\mathbf{P}_t^-\mathbf{H}^T + R\right)^{-1} . \tag{12}$$

$$\mathbf{x}_t^+ = \mathbf{x}_t^- + \mathbf{K}_t\left(Q_t^o - \mathbf{H}\mathbf{x}_t^-\right) . \tag{13}$$

$$\mathbf{P}_t^+ = \left(\mathbf{I} - \mathbf{K}_t\mathbf{H}\right)\mathbf{P}_t^- . \tag{14}$$

where $\mathbf{K}_t$ is the Kalman gain matrix, $\mathbf{P}$ is the error covariance matrix and Q^0 is the new observation. In this study, the observed value of streamflow Q^o is equal to the synthetic CSD estimated as described above. The prior model states $\mathbf{x}$ at time t are updated, as the response to the new available observation, using the analysis equations Eqs. (12) to (14). This allows for estimation of the updated states values (with superscript +) and then assessing the background estimates (with superscript –) for the next time step using the time update equations Eqs. (10) and (11). The proper characterization of the model covariance matrix $\mathbf{S}$ is a fundamental issue in Kalman filter. In this study, in order to evaluate the effect of assimilating CSD, small values of the model error $\mathbf{S}$ are considered for each case study. In fact, a covariance matrix $\mathbf{S}$ with

diagonal values of $1m^6/s^2$, $25m^6/s^2$ and $1m^6/s^2$ are considered for the Brue, Sieve and Alzette catchments. The bigger value of **S** in the Sieve catchment is due to the higher flow magnitude in this catchment if compared to the other two. A sensitivity analysis of model performances depending on the value of **S** is reported in the Results section. For the Bacchiglione catchment, **S** is estimated, for each given flood event, as the variance between observed and simulated flow values.

3.2.2 Assimilation of crowdsourced data

As described in the previous section, a main characteristic of CSDs is to be highly uncertain and to be asynchronous in time. Various methods have been proposed to include asynchronous observations in models. Having reviewed them, in this study we are proposing a somewhat simpler DA approach for integrating Crowdsourced Observations into hydrological models (DACO). This method is based on the assumption that the change in the model states and in the error covariance matrices within the two consecutive model time steps t_0 and t (observation window) is linear, while the inputs are assumed constant. All the CSD received during the observation window are assimilated in order to update the model states and output at time t. Therefore, assuming that one CSD would be available at time t_0^*, the first step of this filter (A in Figure 4) is the definition of the model states and error covariance matrix at t_0^* as:

$$\mathbf{x}_{t_0^*}^- = \mathbf{x}_{t_0}^+ + \left(\mathbf{x}_t^- - \mathbf{x}_{t_0}^+\right) \cdot \frac{t_0^* - t_0}{t - t_0} . \quad (15)$$

$$\mathbf{P}_{t_0^*}^- = \mathbf{P}_{t_0}^+ + \left(\mathbf{P}_t^- - \mathbf{P}_{t_0}^+\right) \cdot \frac{t_0^* - t_0}{t - t_0} \quad (16)$$

The second step (B in Figure 4) is the estimation of the updated model states and error covariance matrix, as the response to the streamflow CSD $Q_{t_0^*}^o$. The estimation of the posterior values of $\mathbf{x}_{t_0^*}^-$ and $\mathbf{P}_{t_0^*}^-$ is performed by Eqs. (13) and (14) respectively. The Kalman gain is estimated by Eq. (12), where the prior values of model states and error covariance matrix at t_0^* are used. Knowing the posterior value $\mathbf{x}_{t_0^*}^+$ and $\mathbf{P}_{t_0^*}^+$ it is possible to predict the value of states and covariance matrix at one model step ahead, t^* (C in Figure 4) using the model forecast equations Eqs. (10) and (11).

The last step (D in Figure 4) is the estimation of the interpolated value of **x** and **P** at time step *t*. This is performed by means of a linear interpolation between the current values of **x** and **P** at t_0^* and t^*:

$$\tilde{\mathbf{x}}_t^- = \mathbf{x}_{t_0^*}^- + \left(\mathbf{x}_{t^*}^- - \mathbf{x}_{t_0^*}^+\right) \cdot \frac{t - t_0^*}{t^* - t_0^*} . \quad (17)$$

$$\tilde{\mathbf{P}}_t^- = \mathbf{P}_{t_0^*}^- + \left(\mathbf{P}_{t^*}^- - \mathbf{P}_{t_0^*}^+\right) \cdot \frac{t - t_0^*}{t^* - t_0^*} . \quad (18)$$

The symbol ~ is added on the new matrices **x** and **P** in order to differentiate them from the original forecasted values in *t*. Assuming that a new streamflow CSD is available at an intermediate time t_1^* (between t_0^* and *t*), the procedure is repeated considering the values at t_0^* and *t* for the linear interpolation. Then, when no more CSDs are available, the updated value of $\tilde{\mathbf{x}}_t^-$ is used to predict the model states and output at *t*+1 (Eqs. (10) and (11)). Finally, in order to account for the intermittent behaviour of this CSD, the approach proposed by Mazzoleni et al. (2015) is applied. In this method, the model states matrix **x** is updated and forecasted when CSDs are available, while without CSD the model is run using Eq. (10) and covariance matrix **P** propagated at the next time step using Eq. (11)

3.2.3 Crowdsourced data accuracy

In this section, the uncertainty related to the CSD is characterised. The observational error is assumed to be the normally distributed noise with zero mean and given standard deviation:

$$\sigma_t^Q = \alpha_t \cdot Q_t^o \quad (19)$$

where the coefficient α is related to the degree of uncertainty of the measurement (Weerts and El Serafy, 2006).

One of the main and obvious issues in citizen-based observations is to maintain the quality control of the water observations (Cortes et al., 2014; Engel and Voshell, 2002). In the Introduction section, a number of methods to estimate (calibrate) the model of observational uncertainty have been referred to. In this study coefficient α is assumed a random variable uniformly distributed between 0.1 and 0.3, so we leave more thorough investigation of uncertainty level of the CSD for future studies. We assumed that the maximum value of α is three times higher than the uncertainty coming from the physical sensors due to the uncertain

estimation of the rating curve at the social sensor location. The value of Q^{true} is the synthetic CSD value measured at an asynchronous time step previously described.

3.3 Experimental setup

In this section, two sets of experiments are performed in order to test the proposed method and assess the benefit of integrating CSD, asynchronous in time and with variable accuracy, in real-time flood forecasting.

In the first set of experiments, called "Experiments 1", assimilation of streamflow CSD at one social sensor location is carried out to understand the sensitivity of the employed hydrological model (KMN) under various scenarios of this data.

In the second set of experiments, called "Experiments 2", the distributed CSD coming from social and physical sensors, at four locations within the Bacchiglione catchment, are considered, with the aim of assessing the improvement in the flood forecasting accuracy.

3.3.1 Experiments 1: Assimilation of crowdsourced data from one social sensor

The focus of Experiments 1 is to study the performance of the hydrological model (KMN) assimilating CSD, having lower arrival frequencies than the model time step and random accuracies, coming from a social sensor located at the outlet point of the Brue, Sieve and Alzette catchments.

To analyse all possible combinations of arrival frequency, number of CSD within the observation window (1 hour) and accuracy, a set of scenarios are considered (Figure 5), changing from regular arrival frequency of CSD with high accuracy (scenario 1) to random and chaotic asynchronous CSD with variable accuracy (scenario 11). In each scenario a varying the number of CSD from 1 to 100 is considered. It is worth noting that for one CSD per hour and regular arrival time, scenario 1 corresponds to the case of physical sensors with an observation arrival frequency of one hour.

Scenario 2 corresponds to the case of CSD having fixed accuracy (α equal to 0.1) and irregular arrival moments, but in which at least one CSD coincides with the model time step. In particular, scenario 1 and 2 are exactly the same for one CSD available within the observation window since it is assumed that the arrival frequency of that CSD has to coincide with the model time step. On the other hand, the arrival frequency of the CSD in scenario 3 is assumed to be random and CSD might not arrive at the model time step.

Scenario 4 considers CSD with regular frequency but random accuracy at different moments within the observation window, whereas in scenario 5 CSD have irregular arrival frequency and random accuracy. In all the previous scenarios the arrival frequency, the number and accuracy of the CSDs are assumed to be periodic, i.e. repeated between consecutive observation windows along all the time series. However this periodic repetitiveness might not occur in real-life, and for this reason, a non-periodic behaviour is assumed in scenarios 6, 7, 8 and 9. The non-periodicity assumptions of the arrival frequency and accuracy are the only factors that differentiate scenarios 6, 7, 8 and 9 from the scenarios 2, 3, 4, and 5 respectively. In addition, the non-periodicity of the number of CSD within the observation window is introduced in scenario 10.

Finally, in scenario 11 the CSD, in addition to all the previous characteristics, might have an intermittent behaviour, i.e. not being available for one or more observation windows.

3.3.2 Experiments 2: Spatially distributed physical and social sensors

Synthetic CSD with the characteristics reported in scenarios 10 and 11 of Experiments 1 are generated due to the unavailability of streamflow CSD at the moment of this study. In order to evaluate the model performances, observed and simulated streamflows are compared, for different lead times.

CSD from physical sensors are assimilated in the hydrological model of AMICO system at an hourly frequency, while CSD from social sensors are assimilated using the DACO method previously described. The updated hydrograph estimated by the hydrological model is used as the input into Muskingum-Cunge model used to propagate the flow downstream, to the gauged station at Ponte degli Angeli, Vicenza.

The main goal of Experiments 2 is to understand the contribution of distributed CSD to the improvement of the flood prediction at a specific point of the catchment, in this case at Ponte degli Angeli. For this reason, five different settings are introduced, and represented in Figure 6, corresponding to different types of employed sensors.

Firstly, only the CSD coming from the physical sensor at the Leogra sub-catchment are used to update the hydrological model of sub-catchment B (setting A). Secondly, in setting B, the model improvement for the assimilation of CSD at the same location of setting A is analysed. In setting C only the distributed CSD within the catchment are assimilated into the hydrological model. Then, setting D accounts for the integration of CSD and physical data, contrary to the setting C

where the physical sensor is dropped in favour of the social sensor at Leogra. Finally, setting E considers the complete integration between physical and social sensors in Leogra, Timonchio and Orolo sub-catchments.

4 Results

4.1 Experiments 1: Influence of crowdsourced data on flood forecasting

The observed and simulated streamflow hydrographs at the outlet section of the Brue, Sieve and Alzette catchments with and without the model update (considering hourly streamflow data) are reported in Figure 7 for nine different flood events for 1 hour lead time. As expected, it can be seen that the updated model tends to better represent the flood events than model without updating in all the case studies. However, this improvement it is closely related to the value of the matrix **S**. In fact, increasing the value of **S**, i.e. assuming a less accurate model, force the model towards the observations because more accurate than the model itself. For this reason, a sensitivity analysis on the influence of the matrix **S** on the assimilation of CSD for scenario 1, i.e. coming and assimilated at regular time steps within the observation windows, is reported in Figure 8. The results of Figure 8 are related to the first flood event of the Brue, Sieve and Alzette catchments. Increasing the number of CSD within the observation window results in an improvement of the NSE for different values of model error. However, this improvement becomes negligible for a given threshold value of CSD, which is a function of the considered flood event. This means that the additional CSD do not add information useful for improving the model performance. Overall, increasing the value of the model error **S** tends to increase NSE values as mentioned before. For this reason, in order to better evaluate the effect of assimilating CSD, a small value of **S**, i.e. model more accurate than CSD, is assumed.

In case scenario 1 the arrival frequency is set as regular for different model runs, so the moments and accuracy in which the CSD became available are always the same for any model run. However, for the other scenarios, the irregular moment in which the CSD becomes available within the observation window and their accuracy are randomly selected and change according to the different model runs. This reflects in a random model performances and consequent NSE. In order to remove such random behaviour, different model runs (100 in this case) are carried out, assuming different random values of arrival and accuracy (coefficient α) during each model run, for a given number of CSD and lead time. The NSE value is estimated for each model run,

so μ(NSE) and σ(NSE) represent the mean and standard deviation of the different values of NSE.

For scenarios 2 and 3 (represented using warm, red and orange, colours in Figure 9 and Figure 10 for lead time equal to 24 hours), i.e. random arrival frequency with fixed/controlled accuracy, the average values of NSE, μ(NSE), are smaller but comparable with the ones obtained for scenario 1 for all the considered flood events and case studies. In particular, scenario 3 has lower μ(NSE) than scenario 2. This can relate to the fact that both scenarios have random arrival frequency, however, in scenario 3 CSDs are not provided at the model time step, as opposed to scenario 2. From Figure 10, higher values of σ(NSE), can be observed for scenario 3. Scenario 2 has the lowest standard deviation for low values of CSD due to the fact that the arrival frequency has to coincide with the model time step and this tends to stabilize the NSE. In particular, for an increasing number of CSD, σ(NSE) tends to decrease. However, a constant trend of σ(NSE) can be observed, due to particular characteristics of the flood events, in case of the flood event 1 of Sieve and flood event 2 and 3 of Alzette. It is worth nothing that scenario 1 has null standard deviation due to the fact that CSDs are assumed coming at the same moment with the same accuracy for all 100 model runs.

In scenario 4, represented using blue color, CSDs are considered coming at regular time steps but having random accuracy. Figure 9 shows that μ(NSE) values are lower for scenario 4 than for scenarios 2 and 3. This can be related to the higher influence of CSD accuracy if compared to arrival frequency. High variability in the model performances, especially for low values of CSD, it can be observed in scenario 4 (Figure 10).

The combined effects of random arrival frequency and CSD accuracy is represented in scenario 5 using a magenta color (i.e. the combination of warm and cold colors used for scenarios 2, 3 and 4) in Figure 9 and Figure 10. As expected, this scenario has the lowest μ(NSE) and the highest σ(NSE) values, compared to those reported above.

The remaining scenarios, from 6 to 9, are equivalent to the ones from 2 to 5 with the only difference that are non-periodic in time. For this reason, in Figure 9 and Figure 10, scenarios from 6 to 9 have the same colour of scenarios 2 to 5 but indicated with a dashed line in order to underline their non-periodic behaviour. Overall, it can be observed that non-periodic scenarios have similar μ(NSE) values to their corresponding periodic scenario. However, the smoother μ(NSE) trends can be explained because of the lower σ(NSE) values, which means that model

performances are less dependent on the non-periodic nature of the CSD than their period behavior. Table 1 shows the NSE values and model improvement obtained for the different experimental scenarios during the different flood events. Overall, small improvements are obtained when NSE is already high for 1 CSD as for the Sieve catchment during flood event 2 or the Alzette catchment in the event 2. Moreover, it can be seen that a lower improvement is achieved for scenarios (2, 3, 6 and 7) where arrival frequency is random and accuracy fixed if compared to those scenarios (4, 5, 8 and 9) where arrival frequency is regular and accuracy is random.

In the previous analysis, model improvements are expressed only in terms of NSE. However, statistics such as NSE only explain the overall model accuracy and not the real increases/decreases in prediction error. Therefore, increases in model accuracy due to the assimilation of CSD have to be presented in different ways as increased accuracy of flood peak magnitudes and timing. For this reason, additional analyses are carried out to assess the change in flood peak prediction considering 3 peaks occurred during flood event 2 in Brue catchment (see Figure 7). Errors in the flood peak timing, Err_t, and intensity, Err_I, are estimated as:

$$Err_t = t_P^o - t_P^S . \tag{20}$$

$$Err_I = \frac{Q_P^o - Q_P^S}{Q_P^o} . \tag{21}$$

where t_p^o and t_p^s are the observed and simulated peak time (hours), while Q_p^o and Q_p^s are the observed and simulated peak streamflow (m^3/s). From the results reported in Figure 11, considering 12-hours lead time, it can be observed that, overall, errors reduction in peak prediction is achieved for increasing number of CSD. In particular, assimilation of CSD has more influence in the reduction of the peak intensity rather than peak timing. In fact, a small reduction of Err_t of about 1 hour is obtained even increasing the number of CSD. In both Err_I and Err_t the higher error reduction is obtained considering fixed CSD accuracy and random arrival frequency (e.g. scenarios 1, 2, 3, 6 and 7). In fact, smaller Err_I error values are obtained for scenario 1, while scenarios 5 and 9 are the ones that show the lowest improvement in terms of peak prediction. These conclusions are very similar to the previous ones obtained analysing only NSE as model performance measures.

The combination of all the previous scenarios is represented by scenario 10, where a changing number of CSD in each observation windows is considered. In scenario 11 the intermittent

nature of CSD is accounted as well. The μ(NSE) and σ(NSE) values of these scenarios obtained for the considered flood events are showed in Figure 12. It can be observed that scenarios 10 tends to provide higher μ(NSE) and lower σ(NSE) values, for a given flood event, if compared to scenarios 11. In fact, intermittency in CSD tends to reduce model performance and increase the variability of NSE values for random configuration of arrival frequency and CSD accuracy. In particular, σ(NSE) tends to be constant for increasing number of CSD.

4.2 Experiments 2: Influence of distributed physical and social sensors

Three different flood events occurred in the Bacchiglione catchment are used for the Experiments 2. Figure 13 shows the observed and simulated streamflow value at the outlet section of Vicenza. In particular, two simulated time series of streamflow are calculated using as input for the hydrological model the measured and forecasted time series of precipitation (provided by AAWA). Overall, an underestimation of the observed streamflow can be observed using forecasted input while the results achieved used measured precipitation tend to well represent the observations. In order to find out what model states leads to a maximum increase of the model performance, a preliminary sensitivity analysis is performed. The four model states, x_S, x_{sur}, x_{sub} and x_L, related to Sw, Q_{sur}, Q_{sub} and Q_g, are perturbed by ±20% around the true state value using the uniform distribution, every time step from the initial time step up to the perturbation time (PT). No correlation between time steps is considered. After PT, the model realizations are run without perturbation in order to assess the perturbation effect on the system memory. No assimilation, and no model update, is performed at this step. From the results reported in Figure 14, related to the flood event 1, it can be observed that the model state x_{sur} is the most sensitive states if compared to the other ones. In addition, the perturbations of all the states seem to affect the model output even after the PT (high system memory). For this reason, in this experiments, only the model state x_{sur} is updated by means of the DACO method.

Scenarios 10 and 11, described in the previous sections, are used to represent the irregular and random behavior of the CSD assimilated in the Bacchiglione catchment.

Figure 15 and Figure 16 show the results obtained from the experiments settings represented in Figure 6 in case of physical and CSD during three different flood events. Three different lead time values are considered. Different model runs (100) are performed to account for the effect induced by the random arrival frequency and accuracy of the CSD within the observation window as described above. From Figure 15, in which CSD have the same characteristics of

previous scenario 10, it can be seen that the assimilation of CSD from the physical sensor in the Leogra sub-catchment (Setting A) provides a better flood prediction at Ponte degli Angeli if compared to the assimilation of a small number of CSD provided by a social sensor in the same location (Setting B). In particular, Figure 15 show that, depending on the flood event, the same NSE values achieved with assimilation of physical data (hourly frequency and high accuracy) can be obtained by assimilating between 10 and 20 CSD per hour for 4 hours lead time. This number of CSD tends to increase for increasing values of lead times. In case of intermittent CSD (Figure 16) the overall reduction of NSE is such that even with a high number of CSD (even higher than 50 per hour) the NSE is always lower than the one obtained assimilating physical streamflow data for any lead time.

For Setting C, it can be observed for all three flood events that distributed social sensors in Timonchio, Leogra and Orolo sub-catchments allow for obtaining higher model performances than the one achieved with only one physical sensor (see Figure 15). However, for flood event 3 this is valid only for small lead time values. In fact, for 8 and 12 hours lead time values, the contribution of CSD tend to decrease in favor of physical data from the Leogra sub-catchment. This effect is predominant for intermittent CSD, scenario 11. In this case, Setting C has higher μ(NSE) values than Setting A only during flood event 1 and for lead time values equal to 4 and 8 hours (see Figure 16).

It is interesting to note that for Setting D, during flood event 1, the μ(NSE) is higher than Setting C for low number of CSD. However, with a higher number of CSD, Setting C is the one providing the best model improvement for low lead time values. In the case of intermittent CSD, it can be noticed that the Setting D provides always higher improvement than Setting C. For flood event 1, the best model improvement is achieved for Setting E, i.e. fully integrating physical sensor with distributed social sensors. On the other hand, during flood events 2 and 3 Setting D shows higher improvements than Setting E. For intermittent CSD the difference between Setting D and E tends to reduce for all the flood events. Overall, settings D and E are the ones which provided the highest μ(NSE) in both scenario 10 and 11. This demonstrates the importance of integrating an existing network of physical sensors (Setting A) with social sensors providing CSD in order to improve flood predictions.

Figure 17 shows the standard deviation of the NSE obtained for the different settings for 4 hours lead time. Similar results are obtained for the 3 considered flood events. In the case of Setting A, σ(NSE) is equal to zero since CSD are coming from the physical sensor at regular time steps.

Higher σ(NSE) values are obtained for Setting B, while including different CSD (Setting C) tend to decrease the value of σ(NSE). It can be observed that σ(NSE) decreases for high values of CSD. As expected, the lowest values of σ(NSE) are achieved including the physical sensor in the DA procedure (Setting D and E). Similar considerations can be drawn for intermittent CSD, where higher and more perturbed σ(NSE) values are obtained.

5 Discussion

The assimilation of CSD is performed in four different case studies considering only one social sensor location in the Brue, Sieve and Alzette catchments, and distributed social and physical sensors in the Bacchiglione catchment.

In the first three catchments, different characteristics of the CSDs are represented by means of 11 scenarios. Nine different flood events are used to assess the beneficial use in assimilating CSD in the hydrological model to improve flood forecasting.

Overall, assimilation of CSD improves model performances in all the considered case studies. In particular, there is a limit in the number of CSD for which satisfactory model improvements can be achieved and for which additional CSD become redundant. This asymptotic behavior, when extra information is added, has also been observed using other metrics by Krstanovic and Singh (1992), Ridolfi et al. (2014), Alfonso et al. (2013)), among others. From Figure 9 it can be seen that, in all the considered catchments, increasing the number of model error induces an increase of this asymptotic value with a consequent reduction of CSD needed to improve model performances. For this reason, a small value of the model error is assumed in this study. In addition, it is not possible to define a priori number of CSD needed to improve model due to the different model behaviour for a given flood event in case of no update. In fact, as reported in Table 1 and Figure 8, flood events with high NSE values even without update tends to achieve the asymptotic values of NSE for small number of CSD (e.g. flood event 1 in Brue and 2 in Sieve), while more CSDs are needed for flood events having low NSE without update. However, for these case studies and during these nine flood events, an indicative value of 10 CSD can be considered to achieve a good model improvement.

Figure 9 and Figure 10 show the μ(NSE) and σ(NSE) values for the scenarios 2 to 9. Figure 9 demonstrate that for irregular arrival frequency and constant accuracy (e.g. scenarios 2, 3, 6 and 7) the NSE is higher than for scenarios in which accuracy is variable and arrival frequency fixed

(e.g. scenarios 4, 5, 8 and 9). These results point out that the model performance is more sensitive to the accuracy of the CSD than to the moment in time at which the streamflow CSD become available. Overall, σ(NSE) tends to decrease for high number of CSD. The combined effects of irregular frequency and uncertainty are reflected in scenario 5 which has the lower mean and higher standard deviation of NSE if compared to the first four scenarios. However, it can be observed from scenarios 2 to 5 that the trend it is not as smooth as the one obtained with scenario 1. This can be related to the fact that NSE may vary with varying arrival frequency and CSD accuracy.

An interesting fact is that passing from periodic to non-periodic scenarios the standard deviation σ(NSE) is significantly reduced, while μ(NSE) remains the same but with a smoother trend. A non-periodic behaviour of the CSD, common in real life, helps to reduce the fluctuation of the NSE generated by the random behaviour of streamflow CSD. Finally, the results obtained for scenarios 10 and 11 are showed in Figure 12. The assimilation of irregular number of CSD in scenario 10, in each observation window, seems to provide the same μ(NSE) than the ones obtained with scenario 9. One of the main outcomes is that the intermittent nature of the CSD (scenario 11) induces a drastic reduction of the NSE and an increase in its noise in both considered flood events. All these previous results are consistent across the considered catchments.

In the case of the Bacchiglione catchment, the physical and CSDs are assimilated within a hydrological model to improve the poor flow prediction in Vicenza for the three considered flood events. In fact, these predictions are affected by an underestimation of the 3-days rainfall forecast used as input in flood forecasting practice in this area.

One of the main outcomes of these analyses is that the replacement of a physical sensor (Setting A) for a social sensor at only one location (settings B) does not improve the model performance in terms of NSE for a small number of CSD. Figure 15 and Figure 16 show that distributed locations of social sensors (setting C) can provide higher values of NSE than a single physical sensor, even for a low number of CSD, for regular CSD (scenario 10). For flood event 1, Setting C provides better model improvement than Setting D for low lead time values and high number of CSD. This can be due to the fact that the physical sensor at Leogra provides constant improvement, for a given lead time, while the social sensor tends to achieve better results with a higher number of CSD. This dominant effect of the social sensor, for high number of CSD,

tends to increase for the higher lead times. On the other hand, for intermittent CSD (scenario 11) this effect decreases in particular for flood events 2 and 3.

Integrating physical and social sensors (Setting D and E) induces the highest model improvements for all the three flood events. For flood event 1, assimilation from Setting E it appears to provide better results than assimilation from Setting D. Opposite results are obtained for flood events 2 and 3. In fact, the high μ(NSE) values of setting D, when compared to setting E during these flood events, can be due to the fact that flood events 2 and 3 are characterized by one main peak and similar shape while flood event 1 has two main peaks. From Figure 17 it can be seen that assimilation of CSD from distributed social sensors tends to reduce the variability of the NSE coefficient in both scenarios 10 and 11.

6 Conclusions

This study assesses the potential use of crowdsourced data in hydrological modelling, which is characterised by its irregular availability and its variable accuracy. We demonstrate that even data with these characteristics can improve flood prediction if integrated into hydrological models. This opens new opportunities in terms of exploiting data being collected in current citizen science projects for the modelling exercise. Our results do not support the idea that social-sensors should partially or totally replace the existing network of physical sensors; instead, that these new data should be used to compensate the lack of traditional observations. In fact, in case of a dense network of physical sensors, the additional information from social sensors might not be necessary because of the high accuracy of the hydrological observations derided by physical sensors

Four different case studies, the Brue (UK), Sieve (Italy), Alzette (Luxemburg) and Bacchiglione (Italy) catchments, are considered, and the two types of hydrological models are used. In the Experiments 1 (Brue, Sieve and Alzette catchments) the sensitivity of the model results to the different frequencies and accuracies of the crowdsourced data derived from a hypothetical social sensor at the catchments outlet is assessed. On the other hand, in the Experiments 2 (Bacchiglione catchment), the influence of the combined assimilation of crowdsourced data, coming from a distributed network of social sensors, and existing streamflow data from physical sensors, used in the Early Warning System implemented by AAWA, is evaluated. Due to the fact that crowdsourced streamflow data are not yet available in all case studies, realistic synthetic data with various characteristics of arrival frequency and accuracy are introduced.

Overall, we demonstrated that the results we have obtained are very similar in terms of model behaviour assimilating asynchronous data in all case studies.

In Experiments 1 it is found that increasing the number of crowdsourced data within the observation window increases the model performance even if these data have irregular arrival frequency and accuracy. Therefore, data accuracy affects the average value of NSE more than the moment in which these data are assimilated. The noise in the NSE is reduced when the assimilated data are considered having non-periodic behaviour. In addition, the intermittent nature of the data tends to drastically reduce the NSE of the model for different values of lead times. In fact, if the intervals between the data are too large then the abundance of crowdsourced data at other times and places is no longer able to compensate their intermittency.

Experiments 2 showed that, in the Bacchiglione catchment, the integration of data from social sensors and the single physical sensor can improve the flood prediction even for a small number of intermittent crowdsourced data. In the case of both physical and social sensors located at the same place, the assimilation of crowdsourced data gives the same model improvement than the assimilation of physical data only for a high number and non-intermittent behaviour. Overall, the integration of existing physical sensors with a new network of social sensors can improve the model predictions, as shown in the Bacchiglione case study. Although the cases and models are different, the presented study demonstrated that the results obtained are very similar in terms of model behaviour assimilating asynchronous data.

Although we have obtained interesting results, this work has some limitations. Firstly, the proposed method used to assimilate crowdsourced data is applied to the linear parts of hydrological models. This means that the proposed methodology has to be tested on models with non-linear dynamics. Secondly, while realistic synthetic streamflow data have been used in this study, the developed methodology was not tested with data coming from actual social sensors. Therefore, the conclusions need to be confirmed using real crowdsourced observations of water level. Finally, advancing methods for a more accurate assessment of the data quality and accuracy of data derived from social sensors need to be considered (e.g. developing a pre-filtering module aimed to select only data having good accuracy while discarding the one with low accuracy).

Future work will be aimed to address the limitations formulated above, which will allow for a better characterization of the crowdsourced data, making them a reliable data source for model-based forecasting.

Acknowledgements

This research was partly funded in the framework of the EC FP7 Project WeSenseIt: Citizen Observatory of Water, grant agreement No. 308429. Data used were supplied by the British Atmospheric Data Centre from the NERC Hydrological Radar Experiment Dataset http://www.badc.rl.ac.uk/data/hyrex/ and by the Alto Adriatico Water Authority (Italy). The Authors wish to thank the two anonymous reviewers the Editor for their insightful and useful comments.

References

Abbott, M. B. and Ionescu, F.: On The Numerical Computation Of Nearly Horizontal Flows, J. Hydraul. Res., 5(2), 97–117, doi:10.1080/00221686709500195, 1967.

ABC: ABC's crowdsourced flood-mapping initiative, ABCs Crowdsourced Flood-Mapp. Initiat. [online] Available from: http://www.abc.net.au/technology/articles/2011/01/13/3112261.htm (Accessed 20 January 2016), 2011.

Alberoni, P., Collier, C. and Khabiti, R.: ACTIF Best practice paper - Understanding and reducing uncertainty in flood forecasting, Proceeding Act. Conf., (1), 1–43, 2005.

Alfonso, L.: Use of hydroinformatics technologies for real time water quality management and operation of distribution networks. Case study of Villavicencio, Colombia, M.Sc. Thesis, UNESCO-IHE, Institute for Water Education, Delft, The Netherlands., 2006.

Alfonso, L., He, L., Lobbrecht, A. and Price, R.: Information theory applied to evaluate the discharge monitoring network of the Magdalena River, J. Hydroinformatics, 15(1), 211, doi:10.2166/hydro.2012.066, 2013.

Alfonso, L., Chacon, J. and Pena-Castellanos. G.: Allowing Citizens to Effortlessly Become Rainfall Sensors, in 36th IAHR World Congress edited, The Hague, the Netherlands, 2015.

Arnold, C. P. and Dey, C. H.: Observing-Systems Simulation Experiments: Past, Present, and Future, Bull. Am. Meteorol. Soc., 67(6), 687–695, doi:10.1175/1520-0477(1986)067<0687:OSSEPP>2.0.CO;2, 1986.

Au, J., Bagchi, P., Chen, B., Martinez, R., Dudley, S. A. and Sorger, G. J.: Methodology for public monitoring of total coliforms, Escherichia coli and toxicity in waterways by Canadian high school students, J. Environ. Manage., 58(3), 213–230, doi:10.1006/jema.2000.0323, 2000.

Aubert, D., Loumagne, C. and Oudin, L.: Sequential assimilation of soil moisture and streamflow data in a conceptual rainfall–runoff model, J. Hydrol., 280(1–4), 145–161, doi:10.1016/S0022-1694(03)00229-4, 2003.

Bergström, S.: Principles and confidence in hydrological modelling, Hydrol. Res., 22(2), 123–136, 1991.

Bird, T. J., Bates, A. E., Lefcheck, J. S., Hill, N. A., Thomson, R. J., Edgar, G. J., Stuart-Smith, R. D., Wotherspoon, S., Krkosek, M., Stuart-Smith, J. F., Pecl, G. T., Barrett, N. and Frusher, S.: Statistical solutions for error and bias in global citizen science datasets, Biol. Conserv., 173, 144–154, doi:10.1016/j.biocon.2013.07.037, 2014.

Bordogna, G., Carrara, P., Criscuolo, L., Pepe, M. and Rampini, A.: A linguistic decision making approach to assess the quality of volunteer geographic information for citizen science, Inf. Sci., 258, 312–327, doi:10.1016/j.ins.2013.07.013, 2014.

Buytaert, W., Zulkafli, Z., Grainger, S., Acosta, L., Alemie, T. C., Bastiaensen, J., De BiÃ¨vre, B., Bhusal, J., Clark, J., Dewulf, A., Foggin, M., Hannah, D. M., Hergarten, C., Isaeva, A., Karpouzoglou, T., Pandeya, B., Paudel, D., Sharma, K., Steenhuis, T., Tilahun, S., Van Hecken, G. and Zhumanova, M.: Citizen science in hydrology and water resources: opportunities for knowledge generation, ecosystem service management, and sustainable development, Front. Earth Sci., 2(October), 1–21, doi:10.3389/feart.2014.00026, 2014.

Canizares, R., Heemink, A. W. and Vested, H. J.: Application of advanced data assimilation methods for the initialisation of storm surge models, J. Hydraul. Res., 36(4), 655–674, doi:10.1080/00221689809498614, 1998.

Célleri, R., Buytaert, W., De Bièvre, B., Tobón, C., Crespo, P., Molina, J. and Feyen, J.: Understanding the hydrology of tropical Andean ecosystems through an Andean Network of Basins, [online] Available from: http://dspace.ucuenca.edu.ec/handle/123456789/22089 (Accessed 19 February 2016), 2009.

Cifelli, R., Doesken, N., Kennedy, P., Carey, L. D., Rutledge, S. A., Gimmestad, C. and Depue, T.: The Community Collaborative Rain, Hail, and Snow Network: Informal Education for Scientists and Citizens, Bull. Am. Meteorol. Soc., 86(8), 1069–1077, 2005.

Clark, M. P., Rupp, D. E., Woods, R. A., Zheng, X., Ibbitt, R. P., Slater, A. G., Schmidt, J. and Uddstrom, M. J.: Hydrological data assimilation with the ensemble Kalman filter: Use of streamflow observations to update states in a distributed hydrological model, Adv. Water Resour., 31(10), 1309–1324, doi:10.1016/j.advwatres.2008.06.005, 2008.

Cortes Arevalo, V. J., Charrière, M., Bossi, G., Frigerio, S., Schenato, L., Bogaard, T., Bianchizza, C., Pasuto, A. and Sterlacchini, S.: Evaluating data quality collected by volunteers for first-level inspection of hydraulic structures in mountain catchments, Nat. Hazards Earth Syst. Sci., 14(10), 2681–2698, doi:10.5194/nhess-14-2681-2014, 2014.

Degrossi, L. C., Do Amaral, G. G., da Vasconcelos, E. S. M., Albuquerque, J. P. and Ueyama, J.: Using Wireless Sensor Networks in the Sensor Web for Flood Monitoring in Brazil, in Proceedings of the 10th International ISCRAM Conference, Baden-Baden, Germany. [online] Available from: http://humanitariancomp.referata.com/wiki/Using_Wireless_Sensor_Networks_in_the_Sensor_Web_for_Flood_Monitoring_in_Brazil (Accessed 10 February 2016), 2013.

878 Derber, J. and Rosati, A.: A Global Oceanic Data Assimilation System, J. Phys. Oceanogr.,
879 19(9), 1333–1347, doi:10.1175/1520-0485(1989)019<1333:AGODAS>2.0.CO;2, 1989.
880 DHI: MIKE FLOOD User Manual, 2005.
881 Drecourt, J.-P.: Data assimilation in hydrological modelling, Environment & Resources DTU.
882 Technical University of Denmark., 2004.
883 Eckhardt, K.: How to construct recursive digital filters for baseflow separation, Hydrol.
884 Process., 19(2), 507–515, doi:10.1002/hyp.5675, 2005.
885 Engel, S. R. and Voshell Jr, J. R.: Volunteer biological monitoring: can it accurately assess the
886 ecological condition of streams?, Am. Entomol., 48(3), 164–177, 2002.
887 Errico, R. M. and Privé, N. C.: An estimate of some analysis-error statistics using the Global
888 Modeling and Assimilation Office observing-system simulation framework, Q. J. R.
889 Meteorol. Soc., 140(680), 1005–1012, doi:10.1002/qj.2180, 2014.
890 Errico, R. M., Yang, R., Privé, N. C., Tai, K.-S., Todling, R., Sienkiewicz, M. E. and Guo, J.:
891 Development and validation of observing-system simulation experiments at NASA's Global
892 Modeling and Assimilation Office, Q. J. R. Meteorol. Soc., 139(674), 1162–1178,
893 doi:10.1002/qj.2027, 2013.
894 Evensen, G.: Data Assimilation: The Ensemble Kalman Filter, 2nd ed. 2009 edition., Springer,
895 Place of publication not identified., 2006.
896 Fenicia, F., Solomatine, D. P., Savenije, H. H. G. and Matgen, P.: Soft combination of local
897 models in a multi-objective framework, Hydrol. Earth Syst. Sci. Discuss., 4, 91–123,
898 doi:10.5194/hessd-4-91-2007, 2007.
899 Ferri, M., Monego, M., Norbiato, D., Baruffi, F., Toffolon, C. and Casarin, R.: La piattaforma
900 previsionale per i bacini idrografici del Nord Est Adriatico (I), in Proc.XXXIII Conference
901 of Hydraulics and Hydraulic Engineering, p. 10, Brescia., 2012.
902 Giandotti, M.: Previsione delle piene e delle magre dei corsi d'acqua, Servizio Idrografico
903 Italiano, Rome., 1933.
904 Hargreaves, G.H. and Samani, Z.A.: Estimating potential evapotranspiration, J. Irrig. Drain.
905 Div., 108(3), 225–230, 1982.
906 Huang, B., Kinter, J. L. and Schopf, P. S.: Ocean data assimilation using intermittent analyses
907 and continuous model error correction, Adv. Atmospheric Sci., 19(6), 965–992,
908 doi:10.1007/s00376-002-0059-z, 2002.

Hunt, B. R., Kalnay, E., Kostelich, E. J., Ott, E., Patil, D. J., Sauer, T., Szunyogh, I., Yorke, J. A. and Zimin, A. V.: Four-dimensional Ensemble Kalman Filtering, Tellus A, 56(4), 273–277, doi:10.1111/j.1600-0870.2004.00066.x, 2004.

Huwald, H., Barrenetxea, G., de Jong, S., Ferri, M., Carvalho, R., Lanfranchi, V., McCarthy, S., Glorioso, G., Prior, S., Solà, E., Gil-Roldàn, E., Alfonso, L., Wehn de Montalvo, U., Onencan, A., Solomatine, D. and Lobbrecht, A.: D1.11 Sensor technology requirement analysis, Confidential Deliverable, The WeSenseIt Project (FP7/2007-2013 grant agreement no 308429)., 2013.

Ide, K., Courtier, P., Ghil, M. and Lorenc, A. C.: Unifed notation for data assimilation: operational, sequential and variational, J. Meteorol. Soc. Jpn., 75(1B), 181–189, 1997.

ISPUW: iSPUW: Integrated Sensing and Prediction of Urban Water for Sustainable Cities, [online] Available from: http://ispuw.uta.edu/nsf/ (Accessed 19 February 2016), 2015.

Kalman, R. E.: A new approach to linear filtering and prediction problems, J. Basic Eng., 82(1), 35–45, doi:10.1115/1.3662552, 1960.

Krstanovic, P. F. and Singh, V. P.: Evaluation of rainfall networks using entropy: II. Application, Water Resour. Manag., 6(4), 295–314, doi:10.1007/BF00872282, 1992.

Kumar, R., Chatterjee, C., Lohani, A. K., Kumar, S. and Singh, R. D.: Sensitivity Analysis of the GIUH based Clark Model for a Catchment, Water Resour. Manag., 16(4), 263–278, doi:10.1023/A:1021920717410, 2002.

Laio, F., Porporato, A., Ridolfi, L. and Rodriguez-Iturbe, I.: Plants in water-controlled ecosystems: active role in hydrologic processes and response to water stress: II. Probabilistic soil moisture dynamics, Adv. Water Resour., 24(7), 707–723, doi:10.1016/S0309-1708(01)00005-7, 2001.

Li, Z. and Navon, I. M.: Optimality of variational data assimilation and its relationship with the Kalman filter and smoother, Q. J. R. Meteorol. Soc., 127(572), 661–683, doi:10.1002/qj.49712757220, 2001.

Lowry, C. S. and Fienen, M. N.: CrowdHydrology: Crowdsourcing hydrologic data and engaging citizen scientists, GroundWater, 51(1), 151–156, doi:10.1111/j.1745-6584.2012.00956.x, 2013.

Macpherson, B.: Dynamic initialization by repeated insertion of data, Q. J. R. Meteorol. Soc., 117(501), 965–991, doi:10.1002/qj.49711750105, 1991.

Madsen, H. and Cañizares, R.: Comparison of extended and ensemble Kalman filters for data assimilation in coastal area modelling, Int. J. Numer. Methods Fluids, 31(6), 961–981, doi:10.1002/(SICI)1097-0363(19991130)31:6<961::AID-FLD907>3.0.CO;2-0, 1999.

Massart, S., Pajot, B., Piacentini, A. and Pannekoucke, O.: On the merits of using a 3D-FGAT assimilation scheme with an outer loop for atmospheric situations governed by transport, Mon. Weather Rev., 138(12), 4509–4522, 2010.

Matheron, G.: Principles of geostatistics, Econ. Geol., 58(8), 1246–1266, 1963.

Mazzoleni, M., Alfonso, L. and Solomatine, D.: Influence of spatial distribution of sensors and observation accuracy on the assimilation of distributed streamflow data in hydrological modelling, Hydrological Science Journal, doi: 10.1080/02626667.2016.1247211, 2016.

Mazzoleni, M., Alfonso, L., Chacon-Hurtado, J. and Solomatine, D.: Assimilating uncertain, dynamic and intermittent streamflow observations in hydrological models, Adv. Water Resour., 83, 323–339, 2015.

McDonnell, J. J. and Beven, K.: Debates—The future of hydrological sciences: A (common) path forward? A call to action aimed at understanding velocities, celerities and residence time distributions of the headwater hydrograph, Water Resour. Res., 50(6), 5342–5350, doi:10.1002/2013WR015141, 2014.

Moore, R. J., Jones, D. A., Cox, D. R. and Isham, V. S.: Design of the HYREX raingauge network, Hydrol. Earth Syst. Sci., 4(4), 521–530, doi:10.5194/hess-4-521-2000, 2000.

Ragnoli, E., Zhuk, S., Donncha, F. O., Suits, F. and Hartnett, M.: An optimal interpolation scheme for assimilation of HF radar current data into a numerical ocean model, in Oceans, 2012, pp. 1–5., 2012.

Rakovec, O., Weerts, A. H., Hazenberg, P., F. Torfs, P. J. J. and Uijlenhoet, R.: State updating of a distributed hydrological model with ensemble kalman Filtering: Effects of updating frequency and observation network density on forecast accuracy, Hydrol. Earth Syst. Sci., 16(9), 3435–3449, doi:10.5194/hess-16-3435-2012, 2012.

Rakovec, O., Weerts, A. H., Sumihar, J. and Uijlenhoet, R.: Operational aspects of asynchronous filtering for flood forecasting, Hydrol. Earth Syst. Sci., 19(6), 2911–2924, doi:10.5194/hess-19-2911-2015, 2015.

Refsgaard, J. C.: Validation and Intercomparison of Different Updating Procedures for Real-Time Forecasting, Nord. Hydrol., 28(2), 65–84, doi:10.2166/nh.1997.005, 1997.

971 Ridolfi, E., Alfonso, L., Baldassarre, G. D., Dottori, F., Russo, F. and Napolitano, F.: An
972 entropy approach for the optimization of cross-section spacing for river modelling, Hydrol.
973 Sci. J., 59(1), 126–137, doi:10.1080/02626667.2013.822640, 2014.
974 Rinaldo, A. and Rodriguez-Iturbe, I.: Geomorphological Theory of the Hydrological Response,
975 Hydrol. Process., 10(6), 803–829, doi:10.1002/(SICI)1099-1085(199606)10:6<803::AID-
976 HYP373>3.0.CO;2-N, 1996.
977 Rodríguez-Iturbe, I., González-Sanabria, M. and Bras, R. L.: A geomorphoclimatic theory of
978 the instantaneous unit hydrograph, Water Resour. Res., 18(4), 877–886,
979 doi:10.1029/WR018i004p00877, 1982.
980 Roy, H. E., Pocock, M. J. O., Preston, C. D., Roy, D. B. and Savage, J.: Understanding Citizen
981 Science and Environmental Monitoring, Final Report of UK Environmental Observation
982 Framework., 2012.
983 Sakov, P., Evensen, G. and Bertino, L.: Asynchronous data assimilation with the EnKF, Tellus
984 A, 62(1), 24–29, doi:10.1111/j.1600-0870.2009.00417.x, 2010.
985 Seo, D. ., Kerke, B., Zink, M., Fang, N., Gao, J. and Yu, X.: iSPUW: A Vision for Integrated
986 Sensing and Prediction of Urban Water for Sustainable Cities., 2014.
987 Solomatine, D. P. and Dulal, K. N.: Model trees as an alternative to neural networks in
988 rainfall—runoff modelling, Hydrol. Sci. J., 48(3), 399–411,
989 doi:10.1623/hysj.48.3.399.45291, 2003.
990 Szilagyi, J. and Szollosi-Nagy, A.: Recursive Streamflow Forecasting: A State Space Approach
991 - CRC Press Book., 2010.
992 Todini, E.: A mass conservative and water storage consistent variable parameter Muskingum-
993 Cunge approach, Hydrol. Earth Syst. Sci., 11, 1645–1659, 2007.
994 Tulloch, A. I. T. and Szabo, J. K.: A behavioural ecology approach to understand volunteer
995 surveying for citizen science datasets, Emu, 112(4), 313, doi:10.1071/MU12009, 2012.
996 Vandecasteele, A. and Devillers, R.: Improving volunteered geographic data quality using
997 semantic similarity measurements, ISPRS-Int. Arch. Photogramm. Remote Sens. Spat. Inf.
998 Sci., 1(1), 143–148, 2013.
999 Verlaan, M.: Efficient Kalman Filtering Algorithms for Hydrodynamic Models, PhD Thesis,
1000 Delft University of Technology, The Netherlands., 1998.
1001 Weerts, A. H. and El Serafy, G. Y. H.: Particle filtering and ensemble Kalman filtering for state
1002 updating with hydrological conceptual rainfall-runoff models, Water Resour. Res., 42(9), 1–
1003 17, doi:10.1029/2005WR004093, 2006.

1004 Wehn, U., Rusca, M., Evers, J. and Lanfranchi, V.: Participation in flood risk management and
1005 the potential of citizen observatories: A governance analysis, Environmental Science &
1006 Policy, 48, 225-236, 2015
1007 WMO: Simulated real-time intercomparison of hydrological models, World Meteorological
1008 Organization., 1992.
1009 Wood, S. J., Jones, D. A. and Moore, R. J.: Accuracy of rainfall measurement for scales of
1010 hydrological interest, Hydrol. Earth Syst. Sci. Discuss., 4(4), 531–543, 2000.

1011
1012

1013 **Tables**

1014

1015 Table 1. NSE improvements, from 1 to 50 CSD, for different experimental scenarios during the
1016 nine flood events occurred in the Brue, Sieve and Alzette catchments.

Scenario	1	2	3	4	5	6	7	8	9
Brue - event 1	0.126	0.125	0.140	0.243	0.253	0.125	0.144	0.237	0.248
Brue - event 2	0.416	0.413	0.445	0.920	0.902	0.413	0.463	0.841	0.870
Brue - event 3	0.443	0.438	0.472	0.890	0.842	0.440	0.471	0.809	0.822
Sieve - event 1	0.250	0.246	0.228	0.271	0.221	0.247	0.225	0.263	0.237
Sieve - event 2	0.066	0.064	0.067	0.057	0.056	0.064	0.068	0.057	0.060
Sieve - event 3	0.629	0.623	0.632	1.085	1.045	0.625	0.634	1.019	0.995
Alzette - event 1	0.884	0.881	0.883	1.274	1.265	0.882	0.890	1.251	1.342
Alzette - event 2	0.137	0.135	0.135	0.120	0.121	0.134	0.147	0.119	0.135
Alzette - event 3	0.314	0.309	0.305	0.297	0.283	0.310	0.315	0.297	0.281

1017

Figures

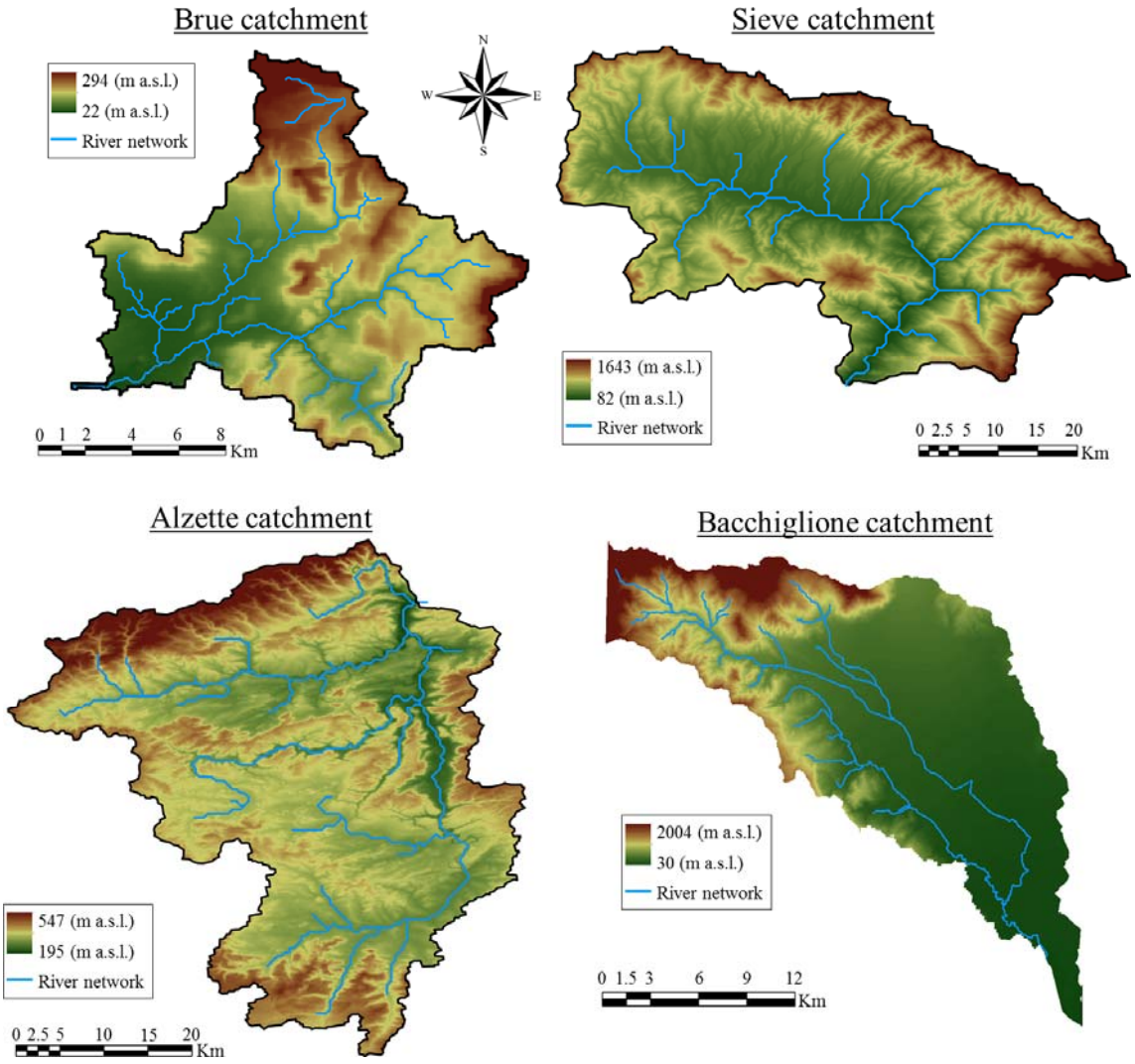

Figure 1. Representation of the four case studies considered in this study

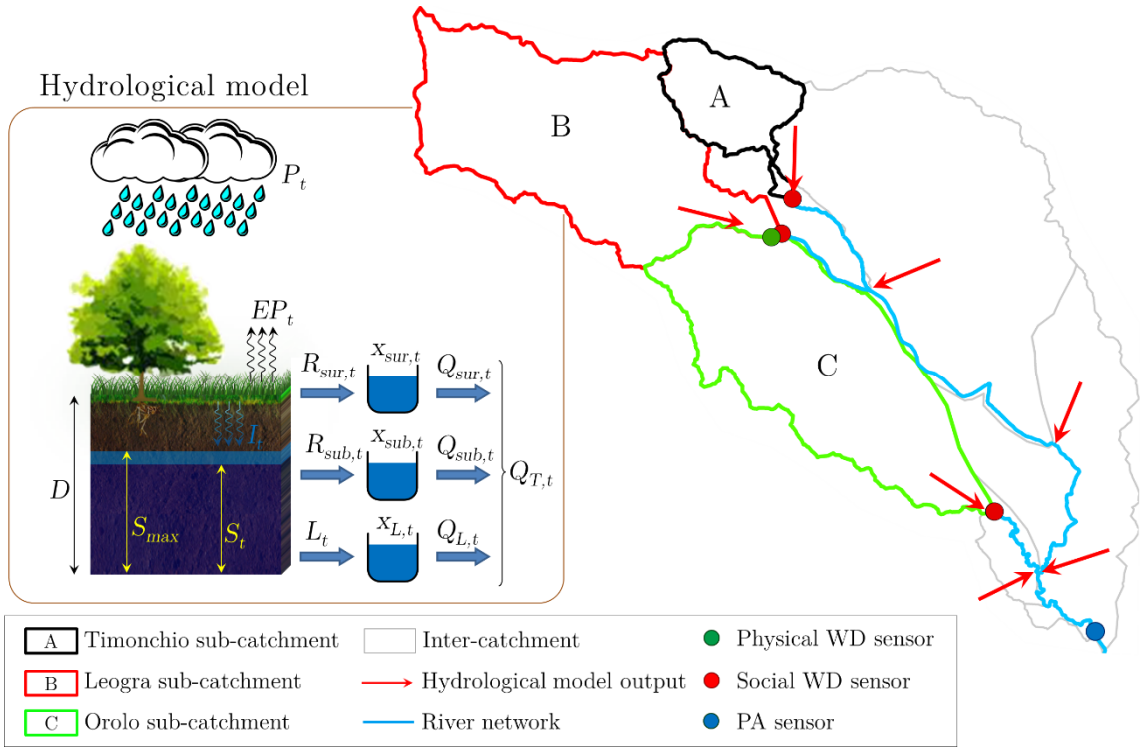

Figure 2. Structure of the early warning system AMICO and location of the physical, social and Ponte degli Angeli (PA) sensors implemented in the Bacchiglione catchment by the Alto Adriatico Water Authority

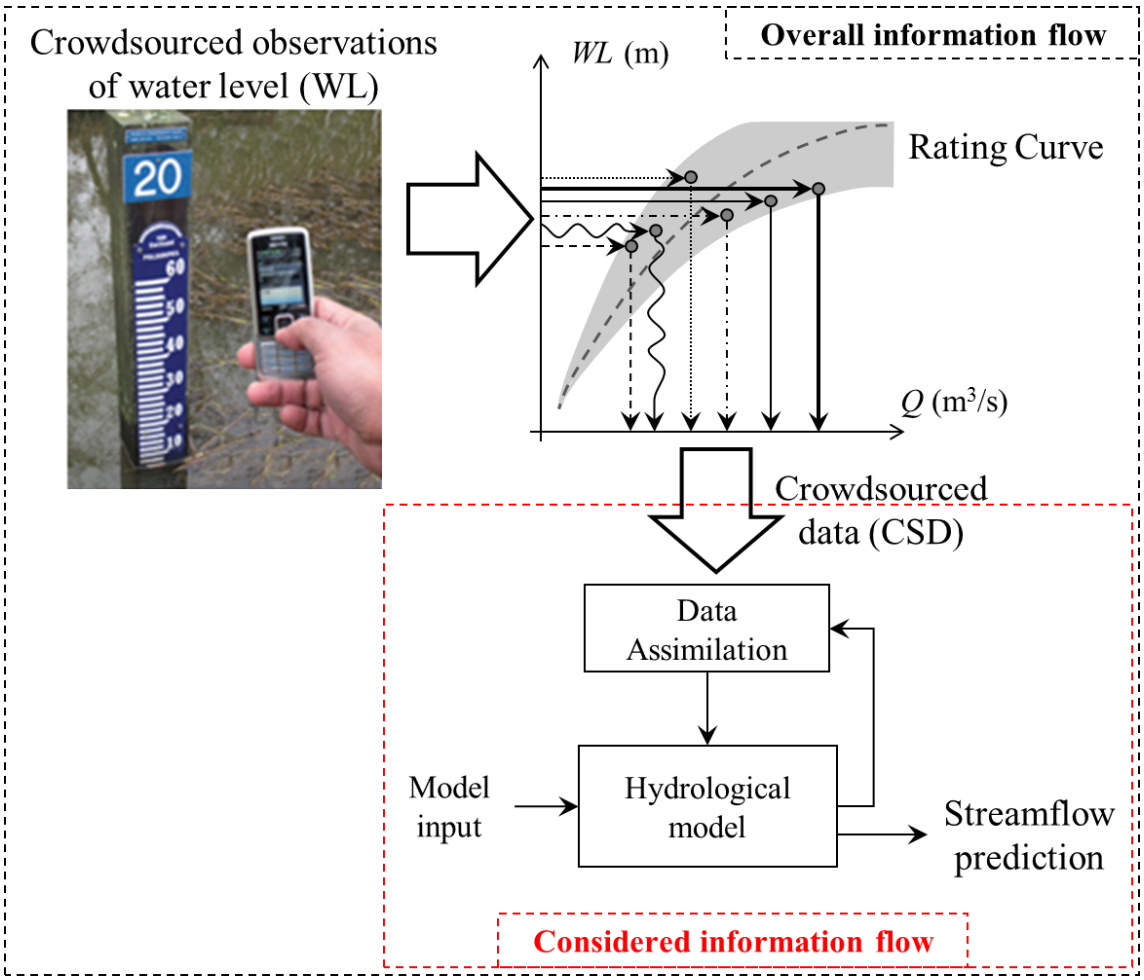

Figure 3. Graphical representation of the methodology proposed to estimate crowdsourced data of streamflow from crowdsourced observations of water level and then assimilate them within hydrological model

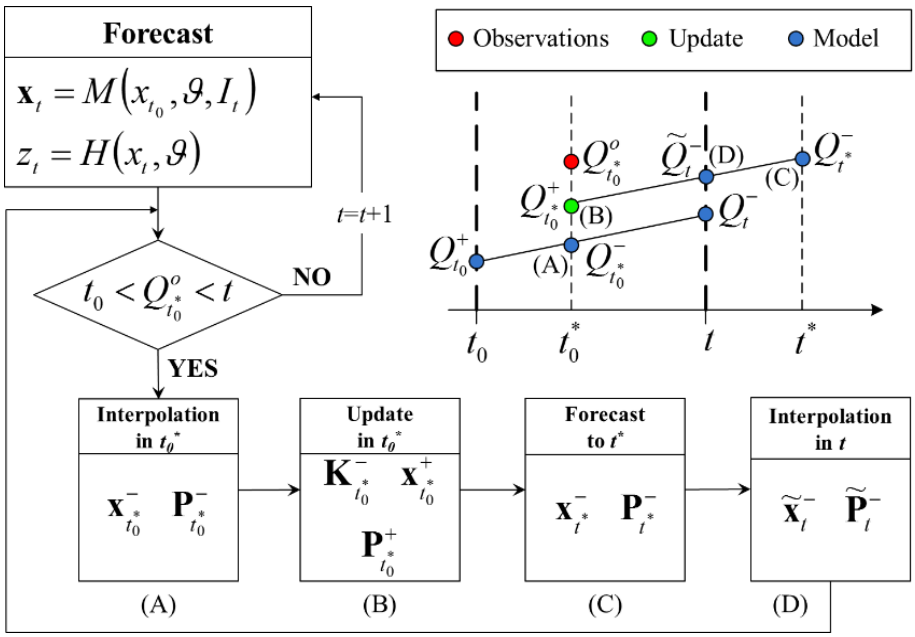

Figure 4. Graphical representation of the DACO method proposed in this study to assimilate asynchronous CSD

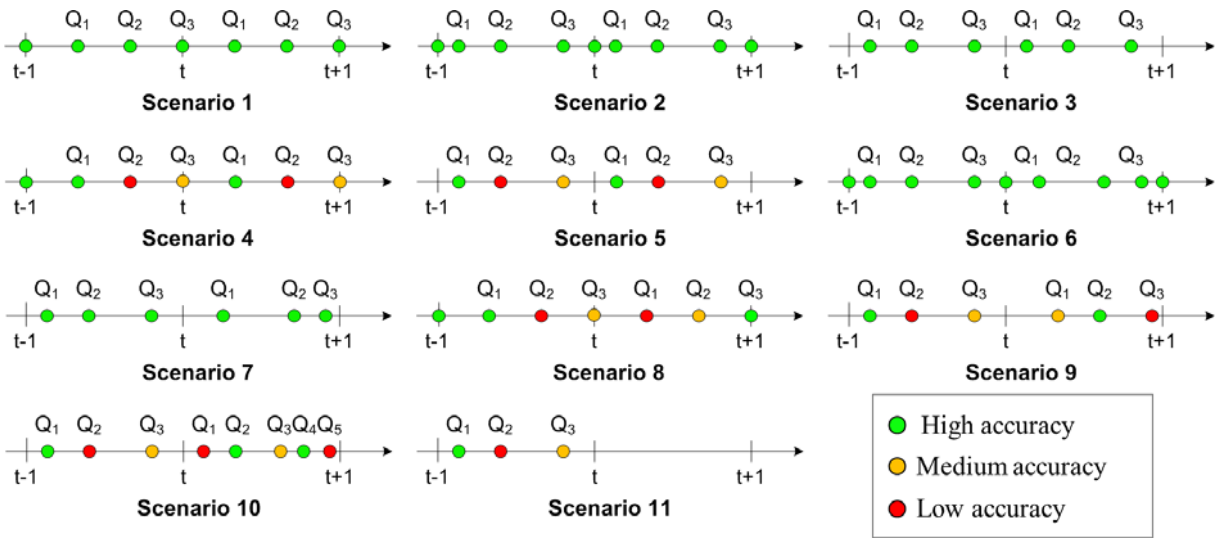

Figure 5. The experimental scenarios representing different configurations of arrival frequency, number and accuracy of the CSD

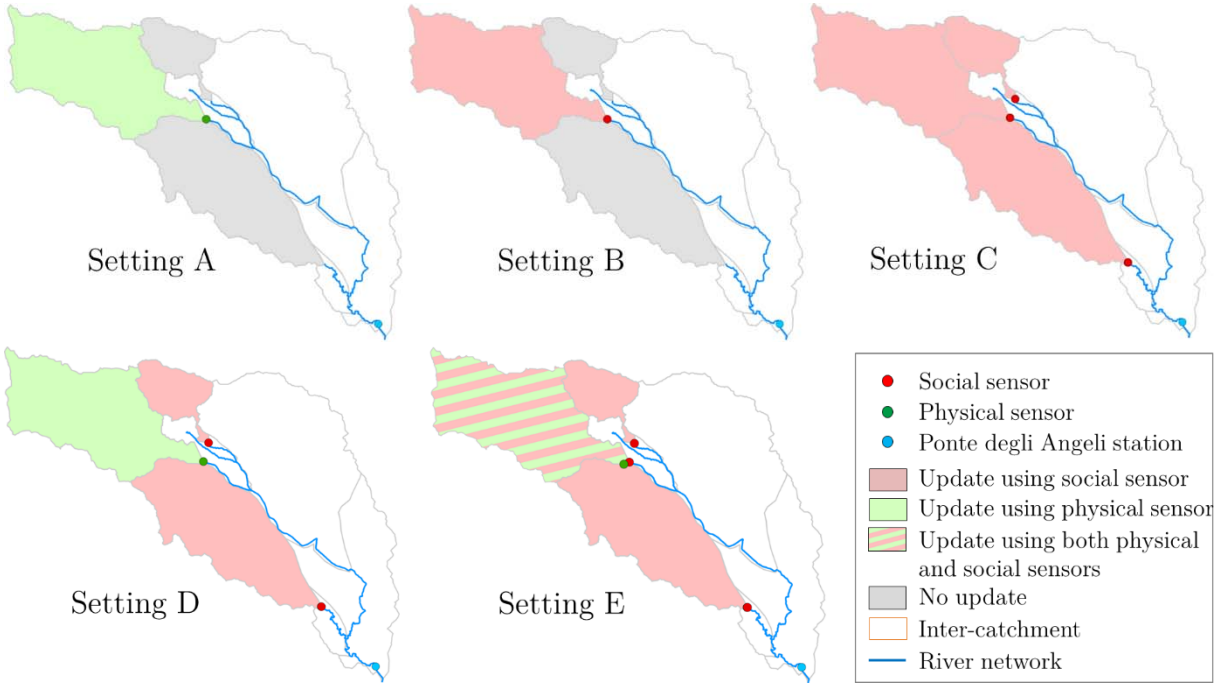

Figure 6. Different experimental settings implemented within the Bacchiglione catchment during Experiments 2

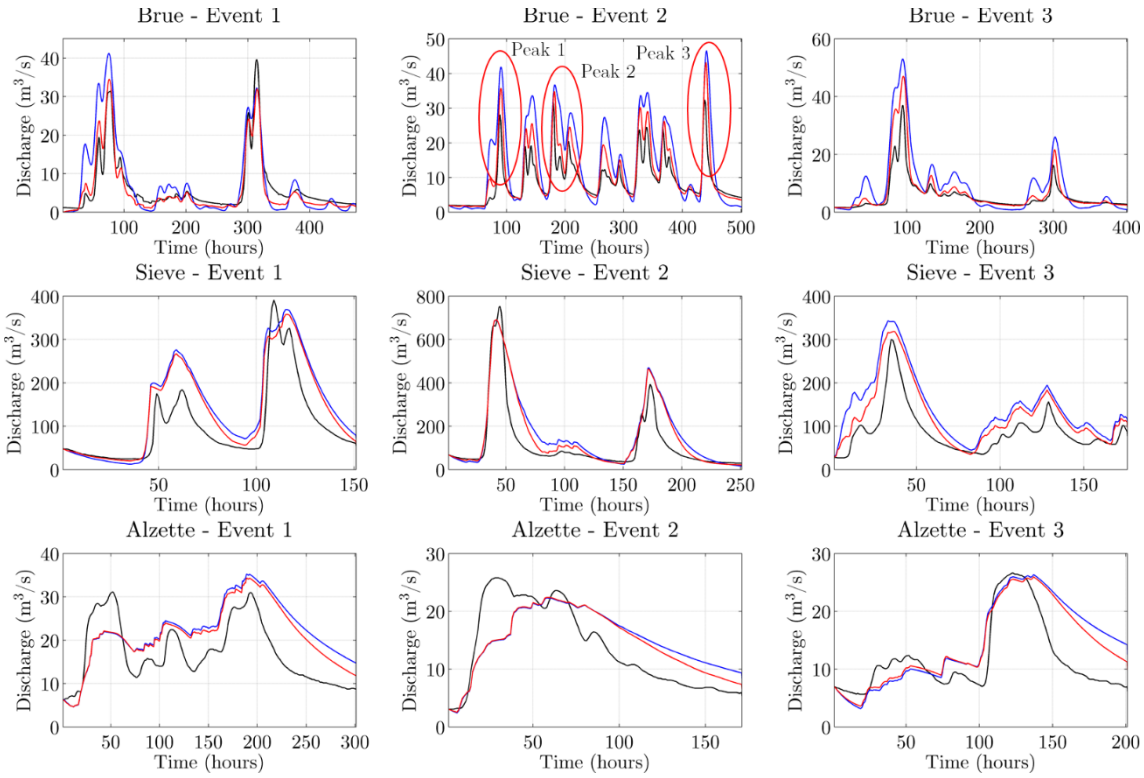

Figure 7. The observed and simulated hydrographs, with and without assimilation, for the nine considered flood events occurred in the Brue, Sieve and Alzette catchments

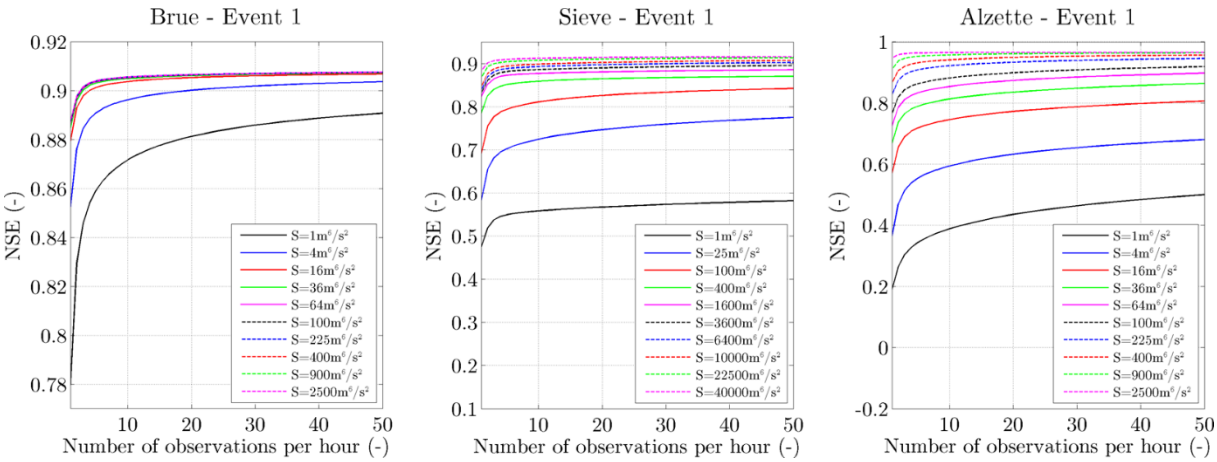

Figure 8. Model improvement in terms of NSE during flood event 1 of each case study, for different values of model error matrix **S** and 24-hours lead time, assimilating streamflow CSD according to scenario 1

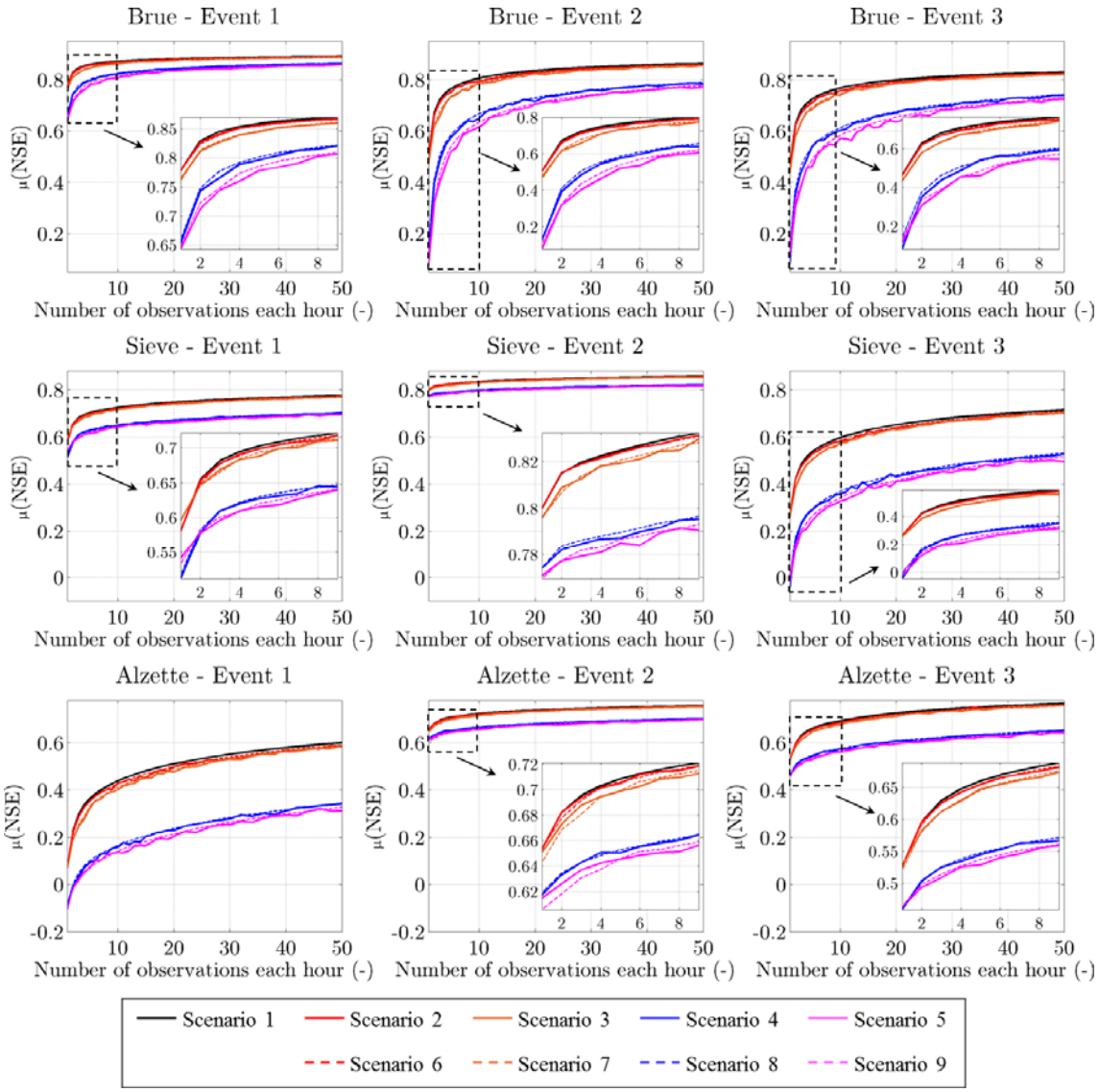

Figure 9. Dependency of μ(NSE) on the number of CSD, for the scenarios 2, 3, 4, 5, 6, 7, 8 and 9 for the five considered flood events

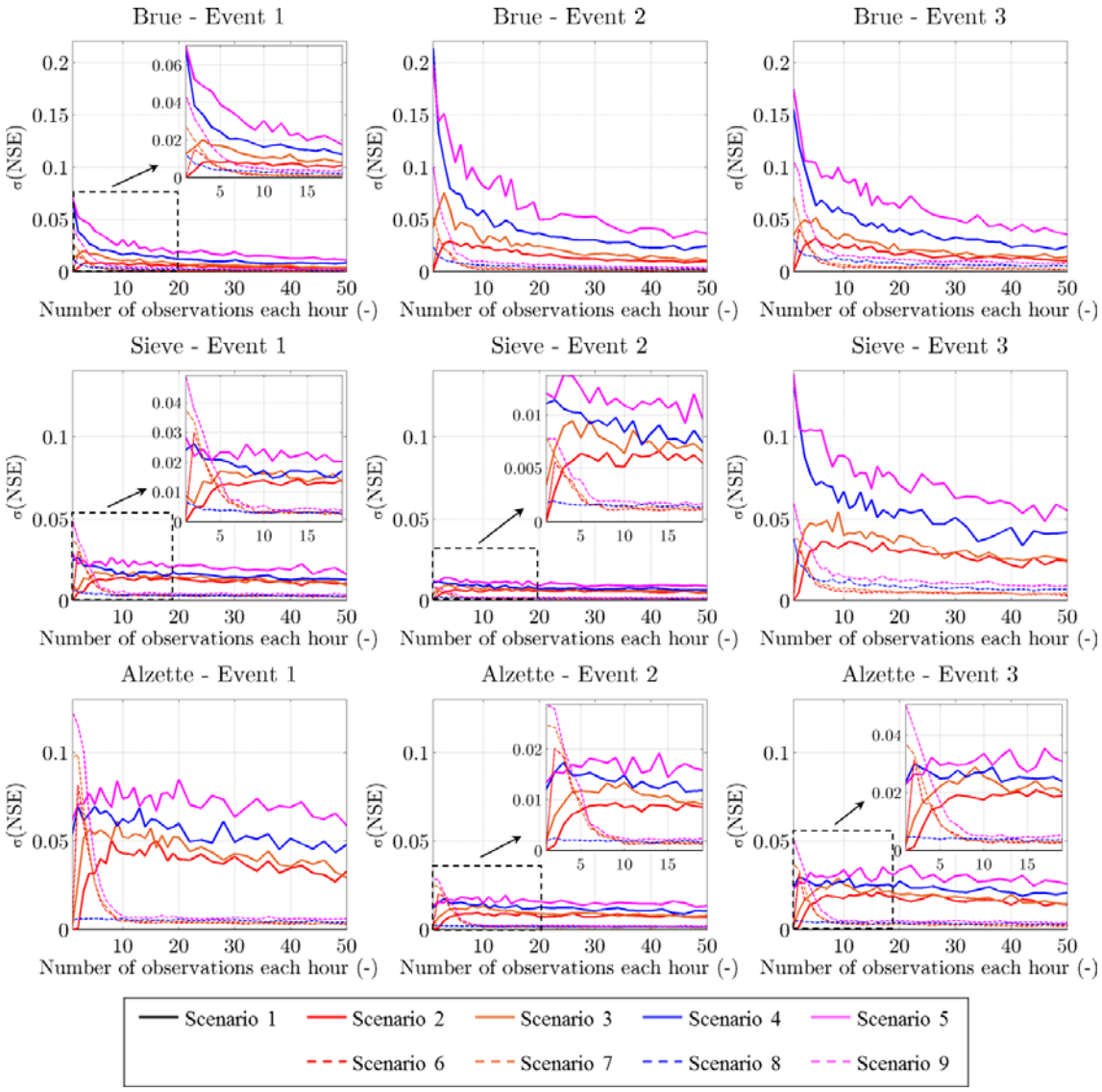

Figure 10. Dependency of σ(NSE) on the number of CSD, for the scenarios 2, 3, 4, 5, 6, 7, 8 and 9 for the five considered flood events

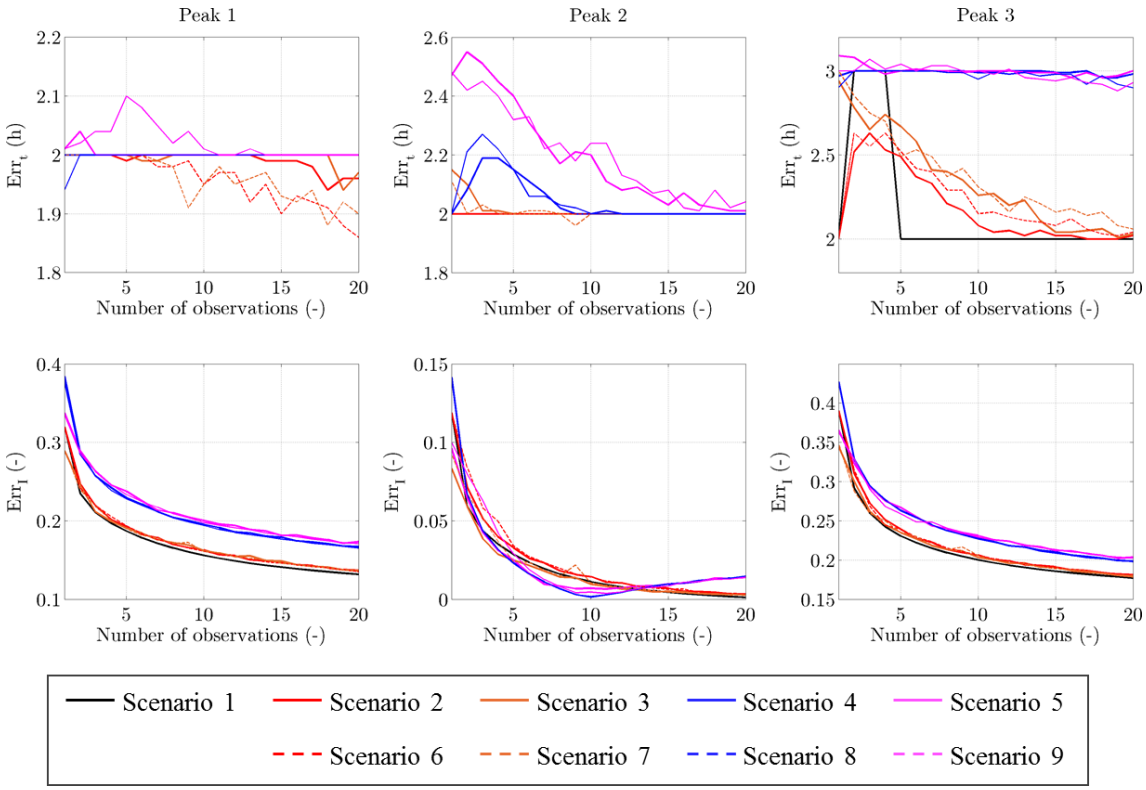

Figure 11. Representation of the Err_t and Err_I as function of number of CSD and experimental scenarios for three different flood peaks occurred during flood event 2 in Brue catchment

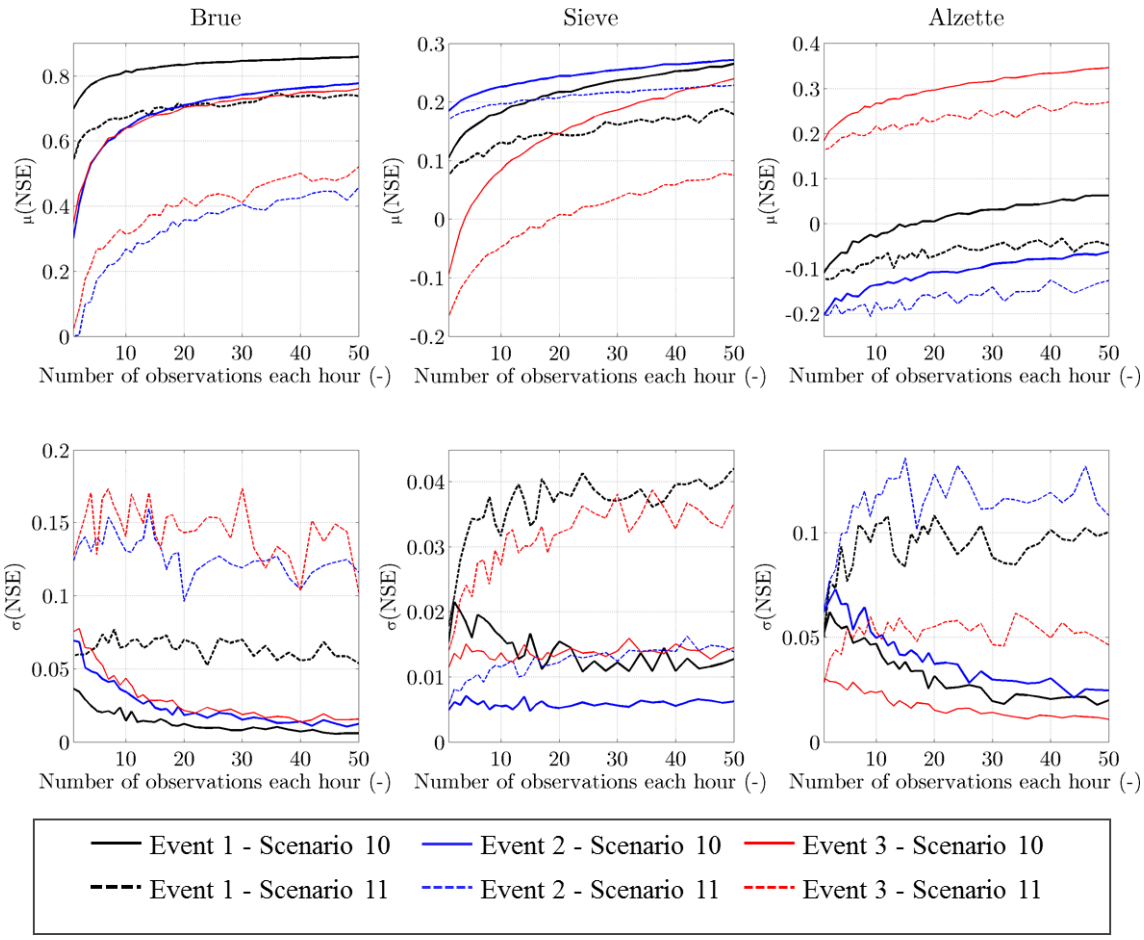

Figure 12. Dependency of the μ(NSE) and σ(NSE) on the number of CSD, for the scenarios 10 and 11 for the five flood events

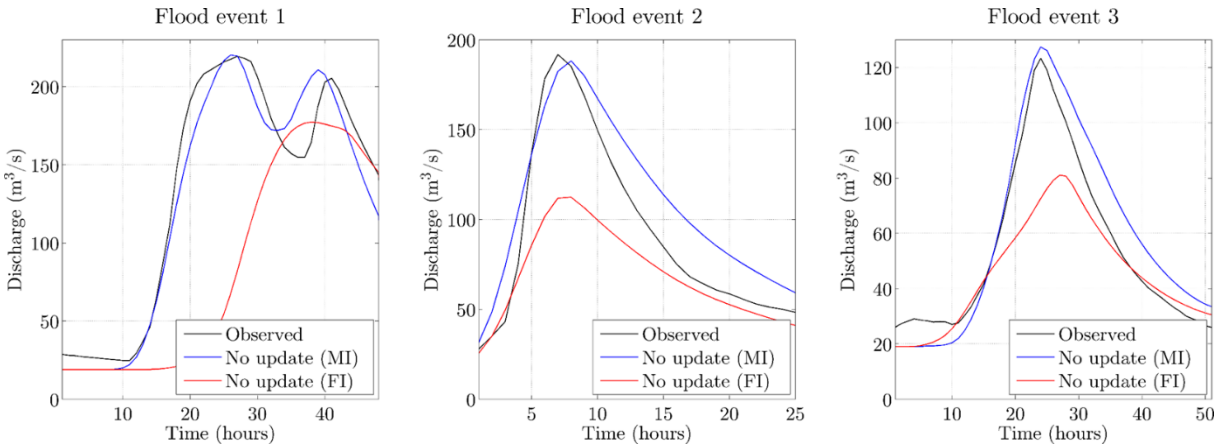

Figure 13. The observed and simulated hydrographs, without update, using measured input (MI) and forecasted input (FI), for the three considered flood events occurred in 2013 (event 1), 2014 (event 2) and 2016 (event 3) on the Bacchiglione catchment

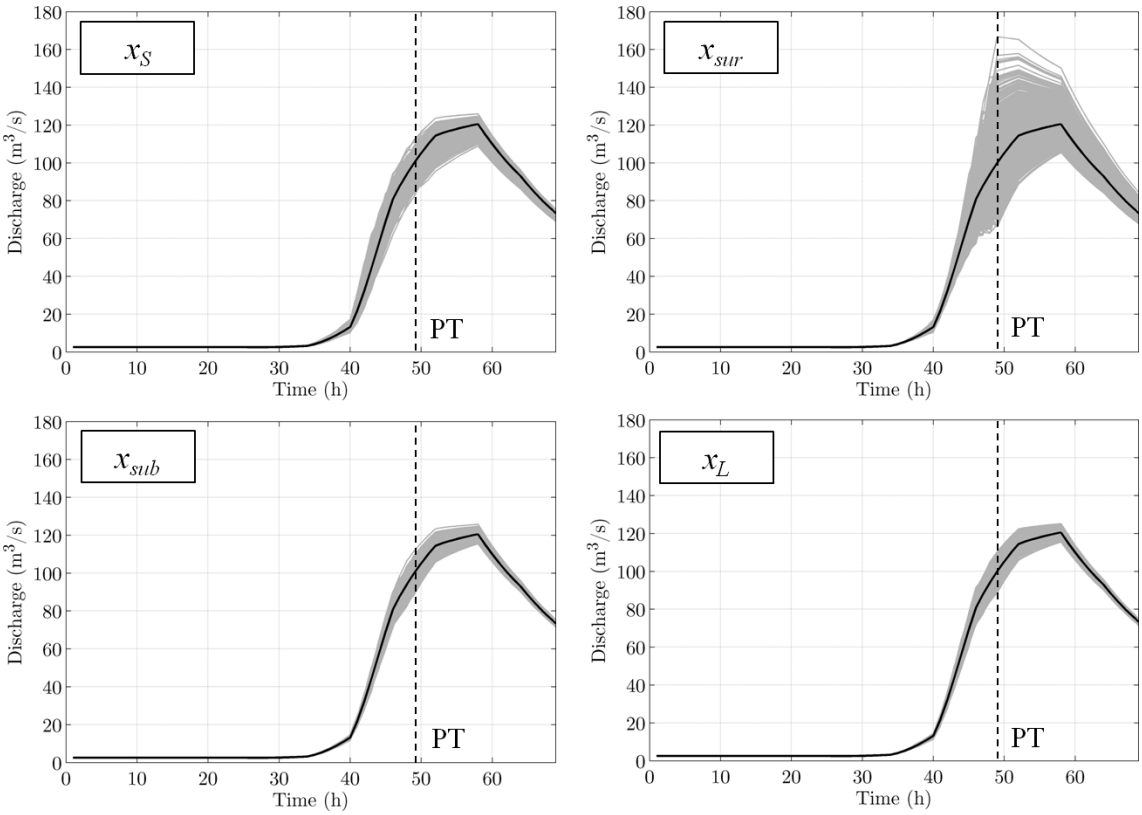

Figure 14. Effect of perturbing the model states on the model output, Bacchiglione case study. PT=Perturbation Time

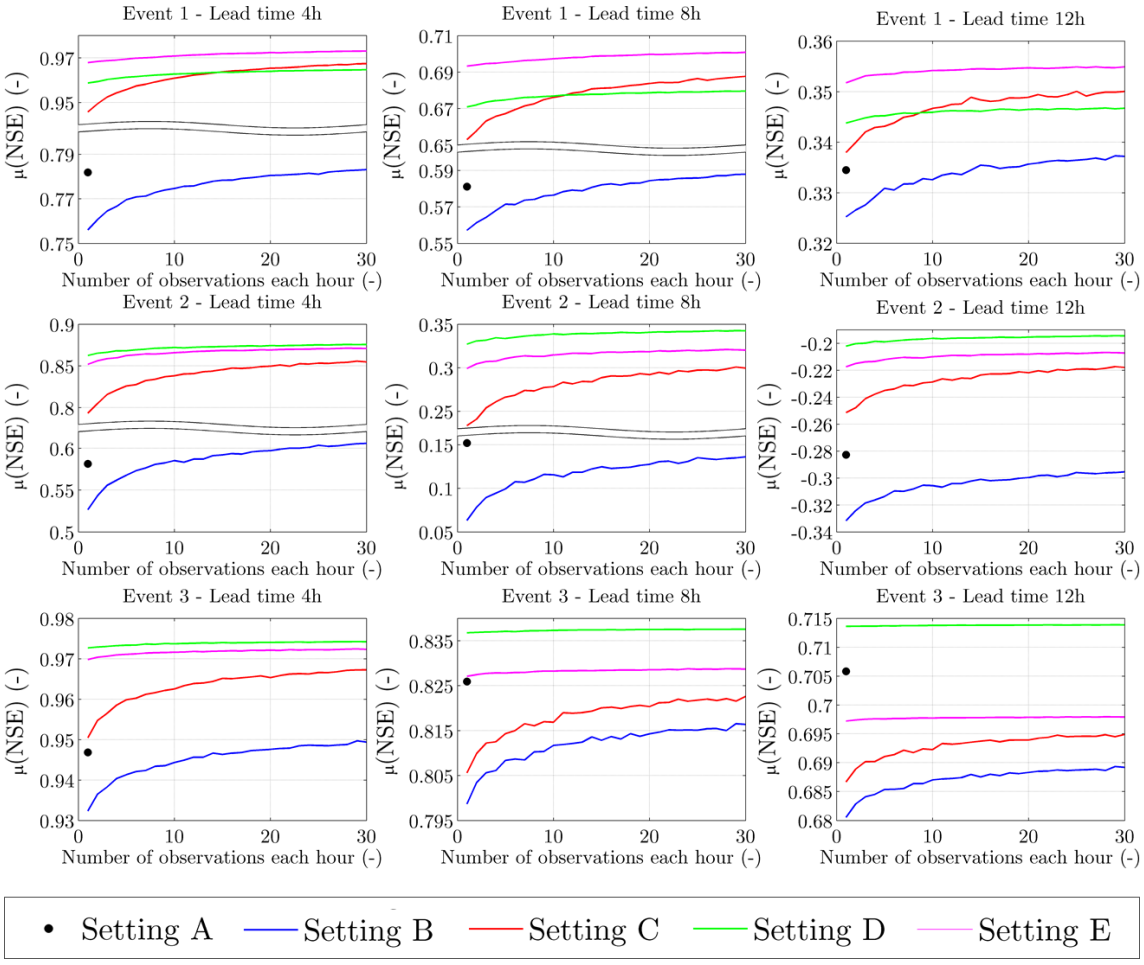

Figure 15. Model performance expressed as μ(NSE) – assimilating different number of CSD during the three considered flood events, for the three lead time values, having characteristic of scenario 10

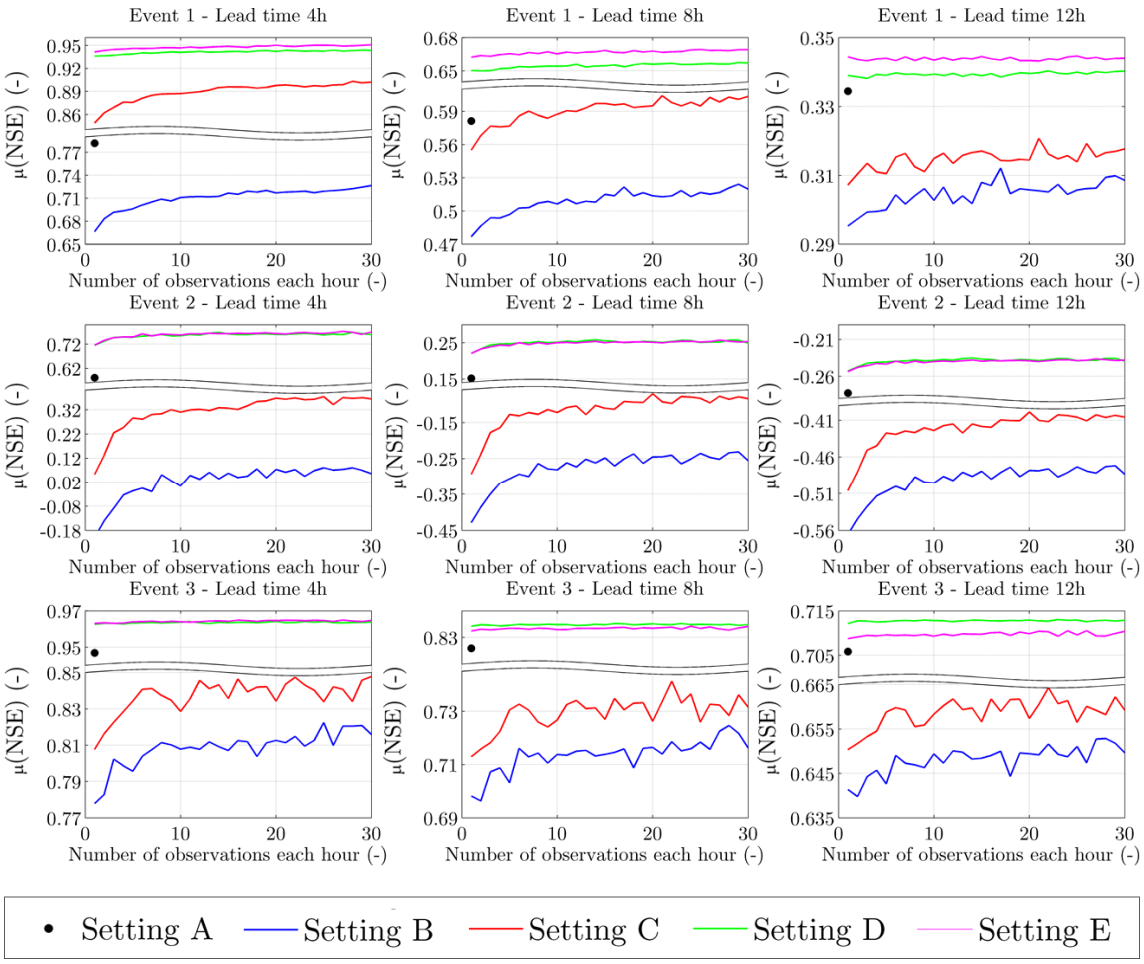

Figure 16. Model performance expressed as μ(NSE) – assimilating different number of CSD during the three considered flood events, for the three lead time values, having characteristic of scenario 11

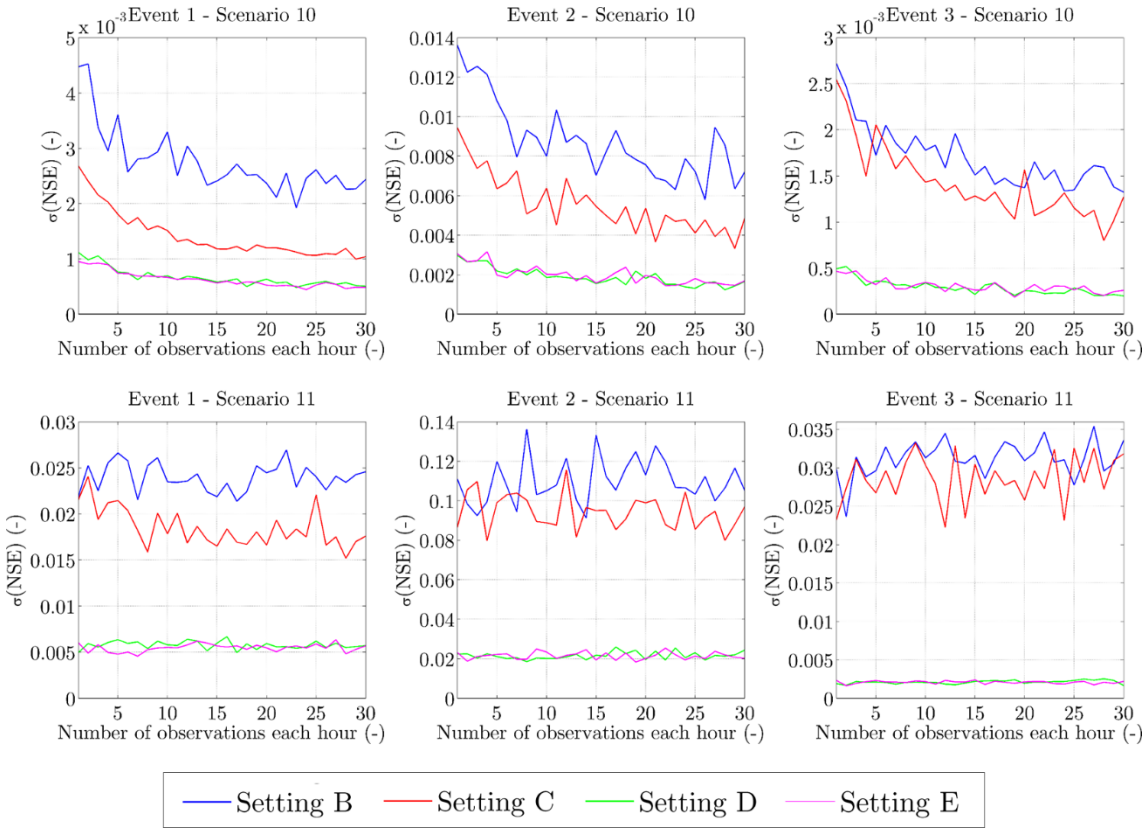

Figure 17. Variability of performance expressed as σ(NSE) – assimilating CSD within setting A, B, C and D, assuming the lead time of 4h, for scenarios 10 and 11 during the three considered flood events